

Developing a Replicable Approach for the Creation of Urban Climatic Maps for Urban Heat  
Island Analysis: A Case Study for the City of Los Angeles, California

by

Bryan Gene Lam

A Thesis Presented to the  
FACULTY OF THE USC DORNSIFE COLLEGE OF LETTERS, ARTS AND SCIENCES  
UNIVERSITY OF SOUTHERN CALIFORNIA  
In Partial Fulfillment of the  
Requirements for the Degree  
MASTER OF SCIENCE  
(GEOGRAPHIC INFORMATION SCIENCE AND TECHNOLOGY)

August 2020

## **Acknowledgements**

I would like to thank Dr. Andrew Marx for his help and guidance into making this project possible, and to Dr. Darren Ruddell and Dr. Steven Fleming for their expertise and comments into shaping and improving this project. I also appreciate the advice Dr. Robert Vos gave me to help steer my project into the right direction. I would also like to thank my coworkers and supervisors at the Los Angeles Department of City Planning and Department of General Services for technical help and for allowing me to use the data necessary for this project. I extend special thanks to Caroline Seymour for her expertise on the urban heat island and to Juan Chavez for his encouragement to pursue this topic. Lastly, I would like to thank my parents for their continued support all these years and am grateful for everything they have done for me.

# Table of Contents

Acknowledgements .....	ii
List of Tables .....	v
List of Figures .....	vi
List of Abbreviations.....	viii
Abstract .....	ix
Chapter 1 - Introduction .....	1
1.1. Motivations .....	1
1.2. Research Objectives .....	5
1.3. Study Area.....	6
1.4. Thesis Organization.....	9
Chapter 2 - Related Work.....	10
2.1. Urban Heat Islands .....	10
2.2. Urban Heat Island Studies in Los Angeles .....	13
2.3. Standardizing Urban Heat Island Studies .....	15
2.4. Urban Climatic Map .....	16
2.5. Urban Heat Island Mitigation Strategies .....	19
Chapter 3 – Methods .....	23
3.1. Data Sources.....	23
3.1.1. Los Angeles Region Imagery Acquisition Consortium Datasets .....	24
3.1.2. Government Datasets .....	25
3.2. Research Design .....	27
3.2.1. Thermal Load Map: .....	29
3.2.2. Dynamic Potential Map:.....	35
3.2.3. Wind Data.....	43

3.2.4. Urban Climatic Map .....	46
3.2.5. Validation and Linear Regression.....	50
Chapter 4 - Results.....	51
4.1. Thermal Load Map .....	51
4.2. Dynamic Potential Map .....	56
4.3. Urban Climatic Map without the Wind Layer .....	64
4.4. Validation/Regression Map.....	66
4.5. Urban Climatic Map with Wind Layer and Prevailing Wind Information.....	70
Chapter 5 - Discussion and Conclusion .....	78
5.1. Observations.....	78
5.2. Limitations .....	81
5.3. Future Work .....	87
5.4. Conclusion .....	92
References .....	93
5.5. Bibliography.....	97

## List of Tables

Table 1: Summary of Government Sourced Datasets .....	26
Table 2: Building Volume Thermal Load Classification (Taken from Ng and Ren 2012) .....	31
Table 3: Elevation Thermal Load Classification (Taken from Ng and Ren 2012).....	33
Table 4: Vegetation Thermal Load Classification (Taken from Ng and Ren 2012) .....	35
Table 5: Ground Coverage Dynamic Potential Classification (From Ng and Ren 2012).....	36
Table 6: Green Space Dynamic Potential Classification (Taken from Ng and Ren 2012).....	38
Table 7: Distance from Coastline Dynamic Potential Classification (From Ng and Ren 2012)...	40
Table 8: Open Space Dynamic Potential Classification (Taken from Ng and Ren 2012).....	41
Table 9: Slope Dynamic Potential Classification (Taken from Ng and Ren 2012).....	42
Table 10: NOAA NCEI Weather Stations .....	44
Table 11: Urban Climate Variable Summary .....	47
Table 12: Urban Climate Classification Descriptions.....	49

## List of Figures

Figure 1: City of Los Angeles .....	7
Figure 2: Los Angeles urban climatic map methodology .....	28
Figure 3: Building Volume Layer Methodology .....	31
Figure 4: Elevation Layer Methodology .....	33
Figure 5: Vegetation Layer Methodology .....	34
Figure 6: Ground Coverage Layer Methodology .....	36
Figure 7: Natural Landscape Layer Methodology .....	38
Figure 8: Proximity to Waterbodies Layer Methodology .....	39
Figure 9: Proximity to Open Spaces Layer Methodology.....	41
Figure 10: Proximity to Open Spaces Layer Methodology.....	42
Figure 11: Example Wind Rose Python script .....	45
Figure 12: Summer 2017 USC Wind Rose in miles per hour .....	46
Figure 13: Building Volume.....	52
Figure 14: Topography.....	53
Figure 15: Vegetation.....	54
Figure 16: Thermal Load Map.....	55
Figure 17: Ground Coverage .....	57
Figure 18: Natural Landscape Cover .....	58
Figure 19: Proximity to Waterfront .....	59
Figure 20: Proximity to Open Spaces .....	60
Figure 21: Vegetated Slopes.....	61
Figure 22: Proximity to Openness .....	62

Figure 23: Dynamic Potential Map.....	63
Figure 24: Draft Urban Climatic Map.....	65
Figure 25: Ordinary Least Squares result for CalEPA UHII and Aggregated Urban Climatic Classes.....	66
Figure 26: Ordinary Least Squares result for CalEPA UHII, Aggregated Urban Climatic Classes, and Projected Wind Speed Values .....	67
Figure 28: Summer Months Wind Roses .....	71
Figure 29: Santa Ana Wind Months Wind Roses.....	72
Figure 30: Weather Station Locations.....	73
Figure 31: Summer Month Wind Roses.....	74
Figure 32: Santa Ana Months Wind Roses .....	75
Figure 33: Final Urban Climatic Map without Wind Layer.....	76
Figure 34: Final Urban Climatic Map with Wind Layer.....	77

## **List of Abbreviations**

CalEPA	California Environmental Protection Agency
ECOSTRESS	Ecosystem Spaceborne Thermal Radiometer Experiment on Space Station
EPA	Environmental Protection Agency
GIS	Geographic Information System
ISA	Impervious Surface Area
LARIAC	Los Angeles Region Imagery Acquisition Consortium
LCD	Local Climatological Dataset
LCZ	Local Climate Zone
LST	Land Surface Temperature
NASA	National Aeronautics and Space Administration
NCEI	National Centers for Environmental Information
NOAA	National Oceanic and Atmospheric Administration
NREL	National Renewable Energy Laboratory
TOC	Transit Oriented Communities
UC/UCM	Urban Climate/Urban Climatic Map
UHI	Urban Heat Island Effect
UHII	Urban Heat Island Index



## **Abstract**

Urbanization and other anthropogenic developments have changed the environments we live in. One of the effects of urbanization is the Urban Heat Island effect, a phenomenon where urbanized areas experience higher temperatures than surrounding rural, less developed areas. While an urban climatic map can be a useful tool for understanding the Urban Heat Island effect, there is not consistent methodology for its creation and implementation in urban planning. This reduces its utility in informing policy and decision making in Urban Heat Island mitigation efforts. In response, this study demonstrates an approach for the creation of accurate urban climatic maps, which can be replicated for all of California. Using the city of Los Angeles as an example, this approach successfully produced different urban climates, and estimates how each urban climate affects the Urban Heat Island effect. The urban climatic map overlays various classified layers from multiple fields, such as urban planning and climatology, to construct the climatic classes for the city. These classification values are based off of the values used in the Hong Kong urban climatic map. Each climatic class is a description of the thermal load and dynamic (air movement) potential that is experienced in each area of the city. Classes with high thermal loads and low dynamic potentials can be identified as areas experiencing a more intense urban heat island effect. Using the same methodology, the creation for additional urban climatic maps, or regional climatic maps is possible, greatly improving regional efforts to mitigate Urban Heat Island effects across California.

## **Chapter 1 - Introduction**

The urban heat island (UHI) effect is a phenomenon in which urbanized areas experience warmer temperatures than surrounding areas due to urbanization and other anthropogenic activities. Warmer temperatures influence the living environments and conditions of more than half of the world's population living in urbanized and developed areas. Researchers have studied the urban heat island extensively and have developed various methods to analyze the causes and effects of the phenomenon. A method used to study the urban heat island effect is using an urban climatic map. Developed by German researchers in the late 20<sup>th</sup> century, the urban climatic map is a useful tool for city planners to visualize the urban morphology of their city and the built environment's potential to contribute to the urban heat island effect. The urban climatic map can be further analyzed by urban planners to recommend best use practices and create policies to mitigate the effects of the urban heat island effect. Population growth, urbanization, and other developments in major cities, such as Los Angeles, are expected to intensify the effects of the urban heat island in the future. The purpose of the urban climatic map is to visualize and analyze the urban heat island effect for Los Angeles, California.

### **1.1. Motivations**

Analyzing the urban heat island effect is crucial in order to understand how urbanization and development can impact its surrounding environment. As a result of increasing urbanization, humans have altered the environment and landscape in a way which affects the microclimates of a region. These effects on the microclimate include altering the region's air and surface temperatures, air pollution levels, and the population's health. It is widely accepted knowledge that the urban heat island effect contributes to heat and pollution retention within a city, which

can have negative implications on the health of the population (Dousset 1992). These effects are intensified through population growth, land use, and other anthropogenic changes within a city. Understanding the causes and effects of the urban heat island is crucial to mitigating the negative warming effects caused by urban development. It is especially important to analyze the urban heat island in major cities, such as Los Angeles, due to its unique geography and past developments which contribute to the effect.

The geography of Los Angeles is a major influence in the temperature variations throughout the city, which can affect the intensities of urban heat island in different regions of the city. Areas along the coast, such as the Westside experience lower temperatures as a result of the constant sea-breeze which blows through the region and cools the region. Inland areas within the Los Angeles Basin, such as South Los Angeles experience much higher temperatures compared to the rest of the city. Other areas, like the San Fernando Valley, typically experience higher temperatures due to the topography, where the Santa Monica Mountains prevents the sea breeze from blowing into the San Fernando Valley. The surrounding mountain ranges effectively forms a shield, preventing cooler air from the ocean to move into the valley.

The topography of Los Angeles also affects the distribution of development within the city, with most of the city's commercial and industrial development found in the flat areas of the Los Angeles Basin. Residential development, on the other hand, are spread out across the various terrain of Los Angeles. The typical commercial and industrial development in the city tend to have a much higher warming potential than residential areas, as there are fewer trees and natural land cover to provide cool areas. Residential areas, especially in hillside communities in the San Fernando Valley, typically contains more trees and more natural land cover, which in turn increases the cooling potential in residential areas. The intensities of urban heat island can differ

based on the geography of the area, and these effects can also be influenced by the different land uses found in the city.

Commercial and industrial development in the city have contributed to making Los Angeles one of the largest cities in the United States, with a majority of the city covered in impervious surfaces, which intensifies the urban heat island effect in these urbanized areas. Anthropogenic materials, such as asphalt and concrete, absorb solar radiation at a much greater rate and quantity than natural land cover such as trees, grasses, and shrubs. The difference in surface energy balance has been well documented in many studies and UHI has been recognized to have an impact in heavily urbanized areas (Arnfield 2003; Taha 1997; Oke 1998). Concentrations of higher density development in regions such as the Downtown area, Wilshire Corridor, contribute to the urban heat island by absorbing solar radiation and retaining the warmer air within the area. Tall buildings, dense urban development, and the limited number of natural spaces in the city also restrict air flow, reducing the ability for cooler air to ventilate the area.

An example of a recent development intensifying the urban heat island effect is the Transit Oriented Communities (TOC) program, intended to provide dense, and affordable housing around transit lines. TOCs are classified based on tiers and are determined based on a location's proximity to a major transit stop and the type of major transit stop. Each tier has different program guidelines, regulations, and incentives to develop affordable housing within these areas (LAMC 12.22 A.31 Sec 6). The taller buildings built under this program have a higher potential to retain heat and restrict air flow to move the warmer air away from the area, intensifying the urban heat island. It is important to study the warming effects caused by urban

development so mitigation strategies can be implemented during the developments' planning phase to lessen the effects of the urban heat island.

Los Angeles has been the study site for many urban heat island studies, and these effects on the city has been well documented. The state of California's Environmental Protection Agency (CalEPA) completed a report which visualized the urban heat island effect in many Californian cities, including Los Angeles. The CalEPA report's methodology followed many other UHI studies, in which the exchanges in water and energy between the atmosphere and the ground and temperature anomalies in an urban setting were analyzed to quantify the UHI effect (Arnfield 2003). Other studies, such as Tran *et al.* (2006), tie the urban heat island effect to urban development, economic, and industrial growth, based on the increase in energy and material consumption. Climatic mapping is another approach in visualizing different microclimates and the urban heat island. These climatic mapping tools can guide planners to better create and develop policies and recommendations to mitigate these effects in the city. Ultimately, the urban climatic map utilizes datasets that are familiar to urban planners, such as land use and building form, which can allow planners better understanding the impacts of the urban heat island.

Urban climatic maps have been developed in other cities around the world including in Europe and Asia. Urban climatic maps were first created in German cities such as Berlin, München (Munich), and Stuttgart in the period between 1970 – 1990. More recent studies have utilized this tool to visualize the urban climate for cities in Asia, such as Tokyo, Kaohsiung, and Hong Kong (Baumüller *et al.* 1992) (Ren *et al.* 2013; Ng *et al.* 2009). Despite its long history and utilization by many cities, an urban climatic map has not been developed for Los Angeles to quantify the effects of UHI in the city.

## 1.2. Research Objectives

The main purpose of the Los Angeles urban climatic map is to quantify the urban heat island effect for the city of Los Angeles, creating an approach that is repeatable assuming required data is available. Analyses includes identifying specific areas of Los Angeles experiencing much more intense urban heat island effect than other areas. One of the possible outputs of the urban climatic map is the quantification and classification of thermal stress and potential for air movement, as shown in the urban climatic map developed by Ng and Ren (2012) for Hong Kong. The results of the urban climatic map can aid urban planners and policy makers in identifying where the most intense urban heat island effects are occurring.

Another objective of the urban climatic map for Los Angeles is to develop a methodology that can be replicated for other regions in Southern California to analyze their urban climates and the potentials for urban heat island. Temperature based urban heat island studies often are specific to a given region due to the variations in the environment. The urban climatic map can be used as the tool to standardize future urban heat island studies in the future, where it takes an urban climate classification approach, rather than a temperature-based approach. Future studies can utilize an urban climatic map to be able to visualize the effects of UHI in proposed future developments, such as those in transit-oriented communities. With this information, urban planners and other policy makers can analyze specific causes and effects of the urban heat island effect at the neighborhood level and propose solutions to mitigate these effects in these specific areas.

While urban climatic maps have been successfully created for multiple cities around the world using similar datasets and variables, replicating one specific model for multiple cities would lead to inaccurate urban classifications. Differences in environment, geographies, and

built environment makes it necessary to use datasets and variables which may be unique to a specific region. As with most cities, the many variables that influence the urban climates and associated microclimates makes modeling these aspects a complex task. It is important to understand that one methodology cannot accurately describe the urban climate of multiple cities around the world. To correct this, the final objective of the urban climatic map for Los Angeles is to identify possible limitations and inaccuracies, and to propose future work to accurately model the urban climate of Los Angeles.

### **1.3. Study Area**

The city of Los Angeles is located in Los Angeles County and serves as the county seat. It is centered around coordinates 34.019394 N, 118.410825 W. The city has a population of approximately 3,990,456 and has an area of approximately 469 square miles/1214 square kilometers (U.S. Census, 2018). The city of Los Angeles is bounded by the Santa Susana Mountains and the San Gabriel Mountains in the north and by the Pacific Ocean along the western and southern portions of the city. A thin corridor connects Los Angeles with the southern coastal areas of San Pedro and Wilmington. The rest of the city is bordered by other cities and unincorporated county areas, which gives the city a unique shape. Figure 1 shows the boundaries of the City of Los Angeles.

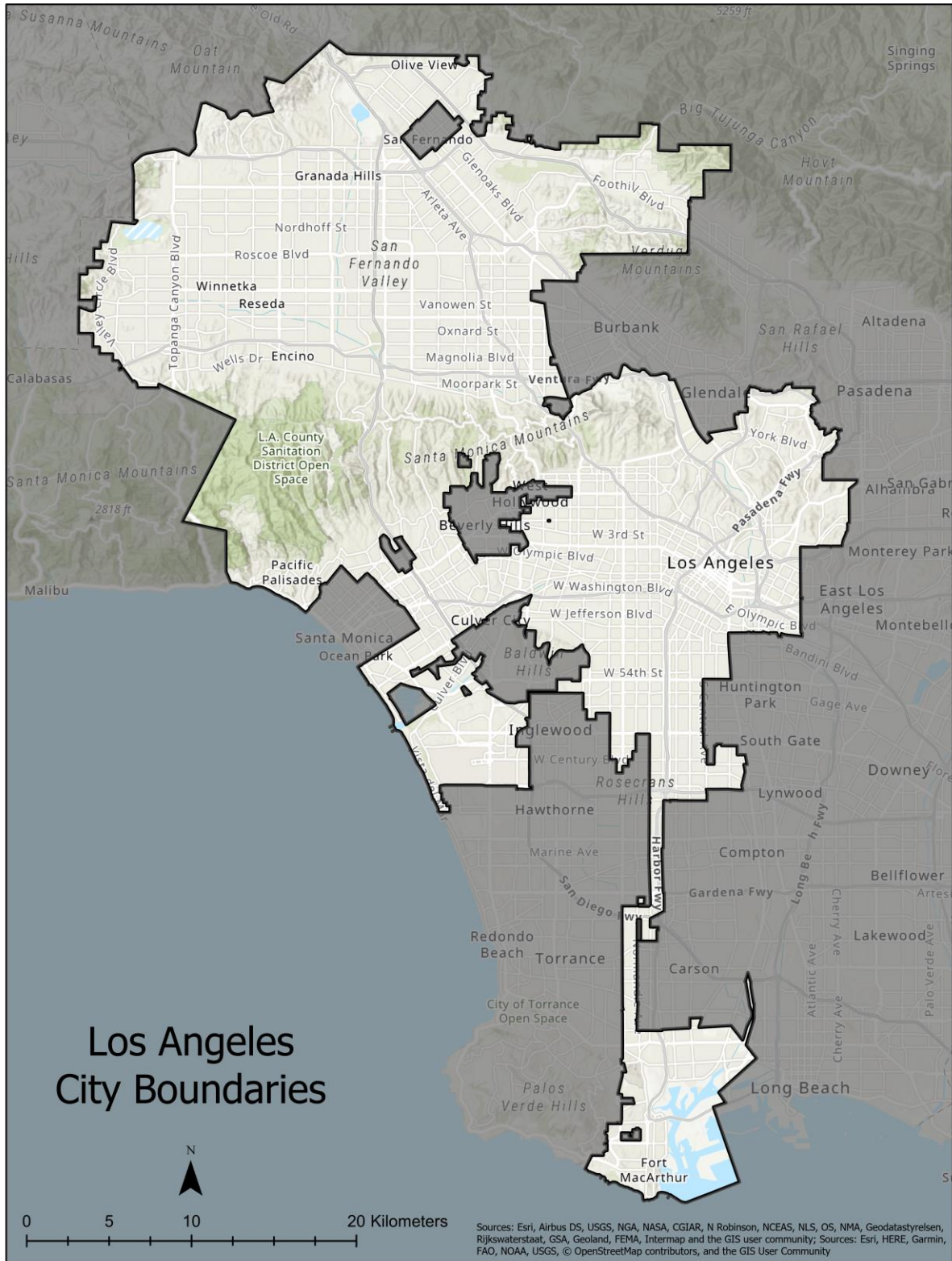


Figure 1: City of Los Angeles



The city's diverse geography allows different types of development found within the city. The mountain, coastal, and basin areas of Los Angeles contains distinct urban development styles. The Los Angeles basin is relatively flat and is where most of the commercial and industrial development in the city is located. The mountain areas within the city of Los Angeles are often preserved and maintained as open spaces or used to develop high-income residential neighborhoods. The terrain makes it difficult to build dense commercial and industrial development typically found in the Los Angeles basin area. The geographic variations found in the city often has various effects on the urban heat island effect observed in the city.

The diversity of the environment can affect the climate of the city. According to the Köppen-Geiger climate classification system, Los Angeles has a Mediterranean climate, characterized by hot, dry summers and mild winter seasons (Peel *et al.* 2007). The seasonal Santa Ana winds also affect the temperatures and humidity during the autumn and early winter months in the city. Santa Ana winds bring extremely dry winds to the Los Angeles region, and often cause wildfires in the mountains surrounding Los Angeles (Westerling *et al.* 2011). Microclimates are also found within the city itself, where temperature ranges can vary from cooler temperatures along the coast to much warmer temperatures found within the San Fernando Valley and in basin neighborhoods such as South Los Angeles.

## **1.4. Thesis Organization**

The proposed thesis is organized into five chapters. Chapter Two reviews a selection of urban heat island studies conducted over many years to provide a background of the urban heat island, the causes of the effect, and the various methodologies that have been proposed to accurately assess the urban heat island effect. This chapter also describes the urban climatic map, its history, and its significance to urban heat island studies. Chapter Three describes the methodology for construction the Los Angeles urban climatic map and the data sources required. Chapter Four presents the results of the urban climatic map and data comparisons to other urban heat island studies. Chapter Five analyzes and discusses the results of the urban climatic map, and their contribution to existing research on urban land cover change over time. It will also contain various limitations of the thesis and presents future work to improve the urban climatic map for Los Angeles.

## **Chapter 2 - Related Work**

The related works chapter reviews various literature to understand the UHI, its significance, and how the urban climatic map can serve as a method for UHI analysis. The chapter is divided into five main sections: (1) A description of the UHI, (2) An analysis of the UHI, (3) The standardization of UHI, (4) The urban climatic map, and (5) Strategies to mitigate UHI. The chapter is aimed to give context and reasoning for the use of the urban climatic map for UHI studies in Los Angeles, California.

### **2.1. Urban Heat Islands**

The urban heat island (UHI) is an urbanized or developed area that experiences higher temperatures than its surroundings. It is the result of anthropogenic changes of the Earth's surface and atmosphere, which allows for the observable temperature differences between urban and rural areas (Oke 1995). The UHI is one of the most studied phenomena and its significance to various Earth System processes, such as climate change, has been well documented. According to Parker (2009), the UHI is one of the main focal points that must be addressed in studies on climate change mitigation strategies. Studies have also analyzed how the UHI can affect the populations living in urban centers, where the increase in temperatures can affect the population's levels of thermal comfort and health.

One of the first studies mentioning the UHI effect was in a study on snowfall frequency in England, where observations of the effects of artificial warming in London and how it may affect the snowfall in the city (Manley 1953). Manley (1953) was one of the first studies to propose the idea of an artificial warming, and the effects on urbanized areas. The study found

that the artificial warming effect may affect the snow frequency observed within the inner London area, but further studies would be needed to support this claim.

In later studies, temperature increases as a result of the UHI can alter climatic patterns in the atmosphere. These climatic patterns can describe conditions such temperature, wind conditions, and precipitation. In a study by Oke (1995), the urban airflow and air pollution found in an urbanized area can influence the ability for clouds to form over a city. As the air heats up due to the UHI, it has a higher potential to contain more water content. When the warmer air rises in the atmosphere, it cools, and the water vapor condenses to produce clouds. Van Heerwaarden and Vilà-Guerau de Arellano (2008) analyzed the effects of urbanization and the UHI on the humidity and the increased ability for heterogeneous surfaces to form clouds. The climatic impacts of UHI as a result of increasing temperatures in cities continue to be a motivation for future UHI studies.

Calculating temperature differences between rural and urban areas are one of the most common methods to quantify the effects of UHI. The calculated temperature differences between urbanized areas and less developed rural areas show that urbanized areas experience warmer temperatures than rural areas due to urban development. These modifications of urban surface causes surrounding air and surface temperatures to rise several degrees higher than the simultaneous temperatures of the surrounding rural areas (Tran *et al.* 2006). Landsberg (1981) also summarizes various UHI studies of cities around the world and finds that temperatures have increased as a result of the growing population and city sizes. The temperature measurements for UHI studies can be measured either through the minimum and maximum temperature differences in an area, or derived from other datasets, such as from specific land cover such as vegetation.

Vegetative cover in a location can affect the temperature of the surrounding environment, as vegetation has a cooling effect on the surrounding environment. The Normalized Difference Vegetation Index (NDVI), a remote sensing index, is one of the most commonly used remote sensing index to quantify the amount of vegetation detected in an area. Since vegetation has the potential to mitigate UHI effects, researchers can use the NDVI to measure temperature changes based on vegetation density. Weng *et al.* (2004) takes a different approach and utilizes a form of vegetation fraction index that is based on land cover type to measure land surface temperatures at the city block level. As a result of urbanization, vegetative land cover is often removed to provide space to build infrastructure. This leads to decreases in effects such as evapotranspiration and solar irradiance, which influence the temperatures in the surrounding area.

Another method of calculating the effects of UHI is the use of surface energy balance models. The variability in how an area can absorb, reflect, and retain solar radiation is the main driver of the UHI effect in a given area. According to Arnfield (2013), soil albedo, moisture availability, and other aspects of the water cycle in the surrounding environment are important components in the surface energy balance and its role in the warming of a region. This would include an increase in solar radiation that is being absorbed by anthropogenic development and the reduction of evapotranspiration rates between the land surface and the atmosphere, which increases temperatures (Kim *et al.* 1992). Altering the environment with anthropogenic infrastructure such as buildings, roads, and other anthropogenic development can lead to solar radiation at a rate much higher than the rate found in rural, open areas.

In other studies, the surrounding biomes and environments were analyzed when studying the causes and effects of the UHI. Imhoff *et al.* (2010) analyzed various cities in the United States and how the different biomes in each city affect the UHI effect in different ways. Using

land surface temperature (LST) data and impervious surface area (ISA) data, they conclude that there is a positive correlation between the intensity of the Urban Heat island effect, the size of the city, and the biome of the city (Imhoff *et al.* 2010). They also concluded that fraction ISA is a good predictor of expected land surface temperatures for all continental U.S. cities in all biomes except deserts and xeric shrublands (Imhoff *et al.* 2010). Tran *et al.* (2006) validates the findings in Imhoff *et al.* (2010) by analyzing various major Asian cities in temperate and tropical climates and found that the UHI intensities were positively correlated to population size of the cities. The distinct climates found in each biome can influence the intensities of the UHI due to specific climatic patterns.

## **2.2. Urban Heat Island Studies in Los Angeles**

In 2012, as part of Assembly Bill 296, the California Environmental Protection Agency (CalEPA) was tasked to develop an index to quantify and visualize the urban heat island effect for various cities around California. Using this index, researchers and policy makers can quantify the urban heat island effect into measurable values and can assess various goals set to mitigate the effects of the urban heat island. This index is based on temperature, in the form of total degree-hours. It is calculated by utilizing variables derived from remote sensing, such as surface reflectance, topography, land use class, and temperature data. The UHII was calculated for each census tract in total degree-hours units (DH) and DH per day averages, in Celsius ( $^{\circ}\text{C}\cdot\text{hr}/\text{day}$ ) (CalEPA 2015). The report described a large range of UHII values in different regions of California and UHII values varied from 2 –  $20^{\circ}\text{C}\cdot\text{hr}/\text{day}$  in smaller urban areas and  $125^{\circ}\text{C}\cdot\text{hr}/\text{day}$  or more in larger urban areas (CalEPA 2015). The report concluded that the cause of the large

variations in UHII values is due to the different microclimates and environments found in each of the cities the report analyzed, such as topography.

One of the regions the CalEPA report analyzed was the Los Angeles Basin. It classified the Los Angeles Basin area as an urban archipelago, which are continuous, large expanses of urban areas, typically bounded by mountains or coastlines (CalEPA 2015). These urban archipelagos act as one large continuous source of heat, rather than multiple pockets of heat that are distributed throughout the city (CalEPA). The report found that the inland regions of the Los Angeles Basin experience a higher UHII due to their distance from the coastline, which brings in sea breezes to cool the region down. UHII values were found to be the highest close to the mountain foothills, at the end of the downwind blowing inland (CalEPA). The models ran for the report found an average air-temperature difference of 6-8°C between inland areas, such as San Bernardino, and coastal cities found to the east of Los Angeles International Airport (LAX) (CalEPA). The UHI effect in the Los Angeles basin is distributed more uniformly, due to the urban archipelago effect causing the warming to be more uniform.

The various land uses within the Los Angeles metropolitan area also affect the intensities of UHI. Most of the Los Angeles region is urbanized, with the distribution of UHI much more equal compared to other cities (Roth *et al.* 1989). However, these UHIs can be detected with the use remote sensing. In their study of Los Angeles, Roth *et al.* 1989 found that all the warm spots identified as UHIs were found in heavily industrial areas and commercial centers, such as South Norwalk and Commerce, which contains industrial buildings and railyards (Roth *et al.* 1989). In another study, Dousset (1992) found similar areas exhibiting intense UHI effects, such as Downtown Los Angeles, Vernon, and Whittier. This is due to the industrial surfaces' ability to absorb solar radiation and warm both the air and the adjacent residential areas. In The two

studies result both conclude that heavily urbanized and cities containing industrial development showed the most intense UHI effect within the Los Angeles region.

### **2.3. Standardizing Urban Heat Island Studies**

The UHI is one of the most studied climatic phenomena, and researchers have calculated and quantified this effect using many different methods. However, there are concerns regarding the accuracy and thoroughness of many UHI studies that have been presented over the years. A study done by Iain Douglas Stewart in 2011 categorized these problems into three different groups: (1) Studies which do not explicitly define UHI and the measurements to quantify UHI; (2) Studies which did not define the difference between urban and rural areas; and (3) Inconsistent methodology (Stewart 2011). The lack of clarity and consistency in many UHI studies mean that it is often difficult to find studies without flaw, as the flaws often question the overall credibility of the study. Stewart's analysis in UHI studies found that around one-half of the UHI studies sampled can be considered credible with complete and competent methodology and reporting (Stewart 2011). Solving this issue would require a methodology which would standardize the criteria for defining urban and rural areas and quantifying the UHI.

The use of a Local Climate Zone (LCZ) map can standardize the methodology for defining urban and rural areas and the quantification of the UHI. One of the first standardized methods for urban climatic studies is the LCZs. It involves classifying a region based on 10 different building types and 7 different land cover types. The UHI is then quantified as the UHI magnitude, the calculation of temperature differences between each LCZ (Stewart & Oke 2012). This approach is used as Stewart & Oke (2012) argue that the urban–rural temperature difference poorly represents the UHI effect as it cannot differentiate between the different surface and



exposure characteristics between the different sample sites (Stewart & Oke 2012). It is often difficult to determine whether the land cover or the buildings found in the urban and rural areas is the main cause of the UHI in a region. Using the LCZ classification system is a relatively simple and inexpensive method to standardize urban climate reporting in any region around the world.

The LCZ model has been successfully utilized for Hong Kong, China, to visualize the built environment. The studies done by Wang *et al.* 2018 and Zheng *et al.* 2018 involved three major steps: (1) Perform sensitivity tests of spatial scale and geolocation of LCZ raster framework, (2) Develop a set of urban morphology/land cover analysis maps and the LCZ classification map at city scale, and (3) Analyze spatial distribution pattern of LCZ classes and quantify urban morphology characteristics for typical LCZ sites (Wang *et al.* 2018; Zheng *et al.* 2018). The resulting LCZ classes were grouped based on a combination of land cover types, such as bare soil and dense tree cover, and land use types, such as agricultural, shrub, or vacant development land. The authors of the two studies produced the LCZ map for Hong Kong to show the urban morphologies of the city and how each LCZ classification can affect the local temperatures.

## **2.4. Urban Climatic Map**

The urban climatic map integrates urban climatic factors and planning policies and considerations together to visualize the urban morphology and its impacts on the local climate (Baumüller *et al.* 1992). The urban climatic map brings another dimension to the traditional LCZ maps by including the topographical, wind, and urban planning aspect to the maps. This includes land use policies, and information on urban infrastructure such as building height, materials, and

footprints, which would affect the local microclimates. The urban climatic map is designed to integrate urban climatology and urban development, two separate disciplines which would benefit users, such as urban planners. These planners can use this map to help make informed urban development decisions for a city.

Building the urban climatic map requires various datasets in order to create an overlay showing the different urban climates of the region. These components include thermal load, dynamic potential, and wind data. The thermal load aspect involves the region's ability to absorb and retain heat, while the dynamic aspect describes the region's ability for air ventilation, to move the heat away from the urbanized areas. While there are many different approaches to building an urban climatic map, the datasets used typically involve an analysis in local air and wind patterns. Wind patterns can include existing and potential air paths, location of barrier effects by buildings, vegetation, or terrain, and various green space information and other urban planning datasets (Ng & Ren 2015). The other datasets used for the urban climatic map are selected based on their impacts to the thermal load and dynamic potential in each city.

The urban climatic map's advantages include the ability to combine climatic knowledge and urban planning recommendations into specific planning policies for a city, such as for master plans, zoning plans, and land use plans (Ng and Ren 2015, 24). Problematic and sensitive areas can be visualized in the urban climatic map, which allows relevant government agencies to take action to mitigate such issues, such as the UHI effect. The simplicity of also makes the urban climatic map easy to communicate the idea of urban climates and other relevant information to the public.

However, there are limitations to the urban climatic map, especially when considering the datasets that the urban climatic map is composed of. As the urban climatic map is

multidisciplinary in nature, it is important to incorporate the expertise and knowledge of urban climatologists in order to fully evaluate the accuracy of the urban climatic map (Ng and Ren 2015, 24). The climate classes categorized by the urban climatic map are also based on land use, and not necessarily an accurate representation of the microclimate at a place in time (Ng and Ren 2015, 24). Urban climate studies must also be done to supplement the urban climatic map in order to accurately define each climate class in the study region. The urban climatic map are focused mainly for urban planning purposes, and as such, must also be presented with planners and land developers' interests in mind.

Urban climate maps have been used as a visualization tool to aid urban climatologists and urban planners around the world. It is not a recent concept and has been successfully utilized by various cities since the late 20<sup>th</sup> century. German researcher Professor Kar Knoch was one of the first researchers to utilize the urban climatic map. He proposed a series of urban climatic maps to be utilized for city planning purposes (Ng and Ren 2015, 11). Later, various German researchers in various cities began to conduct the *Stadtklima*, or 'Urban Climate' in German, as an attempt to mitigate air pollution problems, especially in the Ruhr Valley region in western Germany. Government documents and booklets, such as the one created for the city of Stuttgart, contains information as to the variables that were used to create the UC maps for the city, including climatic, topographic, and urban planning datasets (Baumüller *et al.* 1992). The urban climatic map has since been used in cities of different sizes, such as Yokohama, Japan, Manchester, United Kingdom, and Göteborg, Sweden.

Based on the work done by German urban climatologists, Ng *et al.* (2008) developed an urban climatic map for Hong Kong. Research was done to select the datasets which were appropriate for representing the urban climate of Hong Kong. Ng *et al.* (2008) utilized datasets

including building volume, topography/elevation, green space, ground coverage, natural landscape, and proximity to openness to build the urban climatic map. These variables were ranked based on whether the variables had an intensifying or mitigating effect on the UHI. Once the variables were ranked, the raster datasets were overlaid to create a map with various integer calculations, each representing a different urban climatic class. The different classes are then classified based on their impact on thermal comfort for the region's population. Urban planners can then utilize the different classes visualized by the urban climatic map to create various UHI mitigation plans in Hong Kong.

The flexibility of the urban climatic map allows other cities to include other datasets which can best represent the thermal load and dynamic potentials of the specific cities. The study by Ren *et al.* (2013) created an urban climatic map for Kaohsiung, Taiwan. Similar to the urban climatic map for Hong Kong, the Kaohsiung urban climatic map is based on urban climate studies done by German researchers, with the objective of classifying the climatic variations of the city. However, Ren *et al.* differed from the urban climatic map of Hong Kong as it included a separate layer for waterbodies for the urban climatic map. Waterbodies, such as lakes, ponds, and the coastline found in the city has a cooling effect on its surroundings. The ability to include other variables and datasets into the urban climatic map makes it a flexible tool for urban climate analysis, as the map can be customized based on features of the city, such as the specific topography, climate, or urban development.

## **2.5. Urban Heat Island Mitigation Strategies**

In addition to studies on the causes and effects of UHI, there have been many studies on UHI mitigation strategies in cities. Populations living in these cities affected by UHI are considered vulnerable, as these individuals may not have the capability or access to resources to

adapt and mitigate the harmful effects of UHI. The abnormally warm temperatures can lead to heat stroke and heat exhaustion, especially in the elderly and young, and can lead to increased rates of mortality (Kovats and Hajat, 2008). Lemonsu *et al.* (2015) identified how UHI can be influenced and intensified based on urban planning policies, and other urban expansion strategies based on simulations through an urban canopy model in Paris, France. Using the simulations, Lemonsu *et al.* (2015) found that city densification appears to increase the effects of UHI more than urban sprawl growth. However, the study did note that there were many different factors that could be analyzed individually from the simulations. Lemonsu *et al.* (2015) also concluded it is also difficult to understand which factor may have the most influence in determining the intensity of UHI. Understanding how planning policies, such as land use can unintentionally affect the population by influencing the UHI effects is a key factor in mitigation strategies.

Government agencies, companies, and the public can utilize the knowledge provided in studies to create strategies and policies to mitigate UHI. Recognizing certain parts of the population as particularly vulnerable to UHI would allow organizations, such as the government, to provide them with resources and aid. This can be especially true in poorer neighborhoods, which experience a correlation between higher percentages of poor and minority inhabitants and high heat stress exposure (Harlan *et al.* 2006). Reid *et al.* (2009) also lists other variables which can identify vulnerable populations within a city. This include analyzing demographic, socioeconomic, land cover, preexisting health condition, and air conditioning prevalence data within a certain region. Using this information, researchers can visualize the locations of population most susceptible to urban heat island effects. (Reid *et al.* 2009). Government agencies can also utilize this information to provide policies or inform the public on practices to help mitigate the effects of UHI.

The U.S. Government Environmental Protection Agency (EPA) has published reports to the public with information on UHI and strategies that can be taken to mitigate UHI. This include the use of green and cool roofs and pavements, encouraging the use of urban trees and vegetation, public outreach activities, and at the policy level, where specific tree and landscaping ordinances, building codes, zoning codes, and design guidelines to mitigate the effects of UHI. (U.S. EPA 2012). Santamouris (2019) groups the mitigation technologies into four categories: Reflective and Shading, Greenery, Heat Dissipation, and Anthropogenic Heat Reduction technologies. Each of these categories aim to mitigate different aspects of UHI, such as the heat absorption or heat dissipation aspects.

Studies have also analyzed the effectiveness of these technologies, such as the study done by Solecki *et al.* (2005), which reviewed the technologies and approaches taken by two New Jersey cities to mitigate the effects of UHI. Solecki *et al.* (2005) analyzed the effectiveness of adding urban vegetation and reflective roofs as part of the mitigation strategies in New Jersey. They found that the urban vegetation and reflective roofs are effective at reducing the effects of the UHI. However, less affluent neighborhoods often do not have the resources or open space available to utilize urban vegetation or reflective roofing (Solecki *et al.* 2005). Urban planners and other stakeholders would need to analyze various factors to determine the most effective strategies and technologies for UHI mitigation.

UHI mitigation efforts in Los Angeles would also need to account for air pollution, a significant health hazard to the population of Los Angeles. Rosenfeld *et al.* (1998) analyzes a program in the city to reduce the UHI and indirectly save on energy costs. Reroofing and repaving to lighter colors in the city can reduce the UHI by as much as 3°C (Rosenfeld *et al.* 1998). As part of the 100 Resilient Cities program funded by the Rockefeller foundation, Los

Angeles produced a document which outlines plans and strategies to build resilience against future physical, social, and economic challenges. The resiliency plan for Los Angeles proposes basic planning guidelines which may help mitigate the effects of UHI. This can be used in conjunction with current best use practices and recommendations for specific plan areas to build a UHI mitigation plan that would best help each specific neighborhood.

## **Chapter 3 – Methods**

The methods chapter describes the methods and data sources used to complete the urban climatic map model for Los Angeles. The chapter lists and describes the datasets used to build the urban climatic map, and its usage and significance in the model. The research design section documents the process of building the model for Los Angeles based on urban climate maps completed for other cities. It also includes a brief description of the different urban climatic classes found in the urban climatic map, and the methodology used to create a regression model to validate and compare the urban climatic map with another urban heat island model completed for the Los Angeles region.

### **3.1. Data Sources**

The extent of the urban climatic map of Los Angeles covers the area within city boundaries, which encompasses an area of approximately 1240 square kilometers (479 square miles), according to records from the City of Los Angeles, Bureau of Engineering. The map is composed of classified pixels with data aggregated to 10 square meter resolution, with each pixel covering a 10-meter by 10-meter area. As a result, the majority of the datasets used for the Los Angeles urban climatic map are derived from the 2017 Los Angeles Region Imagery Acquisition Consortium (LARIAC) orthoimagery, captured in the spring of 2017, to take advantage of the high spatial resolution of the imagery. The 10 square meter resolution would result in a model that can visualize the thermal loads and dynamic potentials at a finer scale.



### *3.1.1. Los Angeles Region Imagery Acquisition Consortium Datasets*

The Los Angeles Region Imagery Acquisition Consortium (LARIAC) is composed of many government agencies in the greater Los Angeles area with the goal of acquiring high-resolution imagery for the county. EagleView, the contractor for the LARIAC project, captures imagery approximately every three years, with each capture being a new iteration in the program. There are currently five iterations of the LARIAC program, with LARIAC-5 orthoimagery captured in 2017. As of Spring 2020, imagery collection for LARIAC-6 is currently being captured. For the Los Angeles urban climatic map, the orthoimagery and datasets used is based on the 2017 LARIAC datasets. The imagery dataset is publicly available online through the City of Los Angeles ArcGIS Geohub and the Los Angeles County's GIS portal.

The LARIAC orthoimagery covers the entire extent of Los Angeles County, with a spatial resolution of four inches in urban areas and one-foot resolution in forested and vegetated areas. The orthoimagery is composed of four spectral bands: red, green, blue, and near infrared, and is visualized using a natural color scheme. The orthoimagery is delivered and visualized in GIS software as tiles, with each tile covering an area of approximately ¼ square mile in urban areas and 1 square mile in forested and vegetated areas. The orthoimagery is delivered in the State Plane Coordinate System, NAD83, California, Zone V, U.S. Survey Feet (0405). As the urban climatic map for Los Angeles shares the same projection, the orthoimagery and the derived datasets do not have to be projected to a different coordinate system. The orthoimagery has been checked for quality assurance and is reported to have achieved an accuracy of 1.35 feet with a 95% confidence interval. Other datasets have also been processed and derived from the LARIAC orthoimagery, including layers for building footprint and the elevation contours.

The building footprint layer is a polygon feature class layer which shows the perimeters of the building structure on a property. Fields include the elevation of the building's base and the

height of the building, derived from the LIDAR data collected from the same LARIAC program. Structures with distinguishable roof features and specific heights are also included in the building footprint layer attributes.

The digital elevation model (DEM) is the other dataset derived from the LARIAC orthoimagery. The dataset is available as a contour line layer on the Los Angeles Geohub and is provided at the one-foot, ten-feet, or twenty-feet contour interval. The ArcGIS geoprocessing tool “Topo to Raster” is used to convert the contour data to a raster DEM. The resulting DEM has a spatial resolution of around 9 square feet and has a dimension of 51,686 pixels across by 76,959 pixels in height.

### *3.1.2. Government Datasets*

In addition to the datasets from the LARIAC-5 program, datasets from government sources are also used for the Los Angeles urban climatic map. This includes political boundary layers, the general plan land use, parks layer, the land cover data, and wind data. Excluding the wind dataset and the land cover dataset, all the layers from government sources can be accessed by the public through the Los Angeles ArcGIS Geohub and are available as polygon feature class layers. The land cover dataset is a raster layer derived from the 2017 LARIAC orthoimagery and was created using a supervised classification tool to classify the imagery into eight classification categories: Bare Soil, Buildings, Grass and Shrubs, Roads and Railroads, Tall Shrubs, Tree Canopy, Water, and Other Paved Surfaces. Table 1 is a summary of these datasets.

Table 1: Summary of Government Sourced Datasets

Dataset	Source	Data Type
Los Angeles County Boundary	Los Angeles County Department of Public Works	Polygon feature class
Los Angeles City Boundary	Los Angeles Bureau of Engineering	Polygon feature class
Los Angeles General Plan Land Use	Los Angeles Department of City Planning	Polygon feature class
Los Angeles Parks Layer	Los Angeles Department of Recreation and Parks & Los Angeles Bureau of Engineering	Polygon feature class
Los Angeles Land Cover Layer	Los Angeles Department of City Planning	TIF Raster File
Hourly wind speed and Hourly wind direction	National Oceanic and Atmospheric National Centers for Environmental Information	Comma Separated Values File
Land-Based Wind Speed 80m	United States Department of Energy, National Renewable Energy Labs	TIF Raster File

The wind dataset is collected from the National Oceanic and Atmospheric Administration (NOAA) National Centers for Environmental Information (NCEI). Under the NCEI program, the public can access various climate records, including the Local Climatological Dataset (LCD). The LCD contains hourly, daily, and monthly summaries of climate observations at various weather stations across the United States. These observations include temperature, precipitation, air pressure, and wind data. For the urban climatic map, hourly wind data will be gathered and summarized by season to create wind roses visualizing the prevailing wind conditions during the season. Two fields will be used to construct the wind rose: wind speed and wind direction. The wind speed is the velocity of wind observed given in miles per hour, while wind direction

measures the direction in which the wind is blowing from at any given location. This is measured in directional degrees, with 360° representing north directions and 180° representing south directions. Data recorded with 0° in the directional fields indicate calm wind conditions, which typically describe wind speeds of less than 3 miles per hour.

The Land-Based Wind Speed at 100 meters is provided by the United States Department of Energy, National Renewable Energy Laboratory (NREL). The dataset visualizes projected mean annual wind speed found in a specific area. The original raster layer has a spatial resolution of 2.5 meters and represents wind velocities projected at a 100-meter height. According to the NREL, interpolation methods were used to predict wind speed potential values at a finer resolution. The dataset is visualized as a web-based map, called the “Wind Prospector,” which estimates wind speed potentials across the country.

### **3.2. Research Design**

The Los Angeles urban climatic map methodology emulates the methodology completed for the urban climatic map of Hong Kong by Ng and Ren (2012). The Los Angeles urban climatic map uses the same layers used in the Hong Kong urban climatic map to analyze the thermal loads and dynamic potentials of the city. These layers include building volume, topography, green spaces, ground coverage, natural landscapes, and proximity to openness. The Los Angeles urban climatic map also uses the same classification values as the Hong Kong urban climatic map to classify the impacts each layer has on the thermal loads and dynamic potentials. Ng and Ren (2012) created an additional wind layer using meteorological data and wind models to analyze the prevailing wind and air ventilation conditions for Hong Kong. Due to the time frame of the project, meteorological data is used to construct wind arrows to visualize prevailing

wind conditions for Los Angeles. Figure 2 visualizes the methodology based on the work done by Ng and Ren (2012).

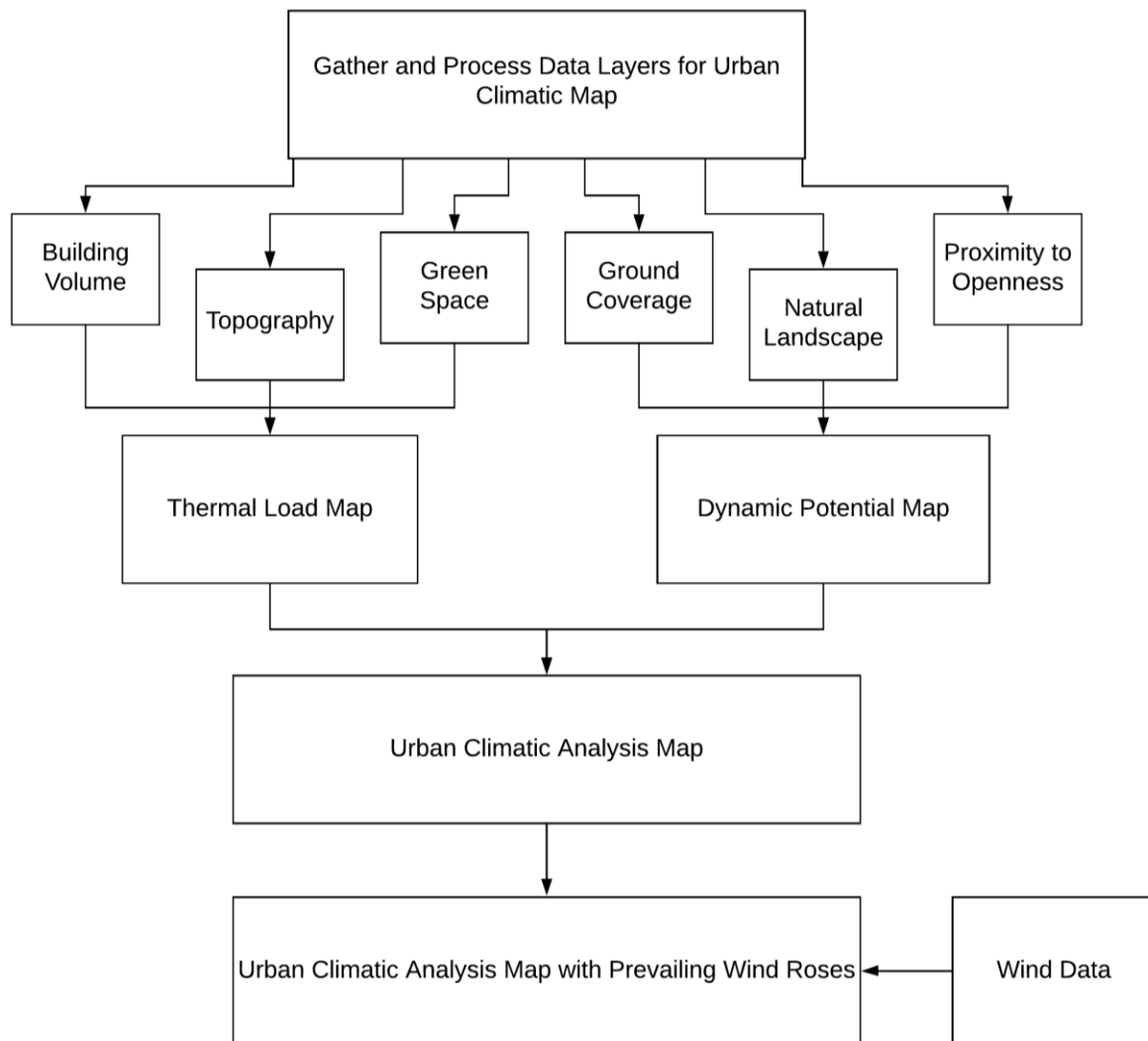


Figure 2: Los Angeles urban climatic map methodology

### *3.2.1. Thermal Load Map:*

The thermal load aspect of the urban climatic map describes the region's ability to absorb and retain heat within an urbanized area. According to Evans and de Schiller (1996), these thermal loads are the variations in urban air temperatures due to the surfaces and urban forms found in the region. Urban forms, which include anthropogenic structures such as commercial buildings and paved asphalt surfaces, can influence the amount of solar radiation that is absorbed and retained within a given area. Three separate layers are created as components to the thermal load layer, which include building volume, topography, and green space.

#### *3.2.1.1. Building Volume*

The building volume layer is used as a measurement of the potential heat that a specific building can retain. A larger building volume results in a higher potential heat capacity, which can be represented within the thermal load layer. The heights of tall urban structures can also obstruct the open sky from the ground level. This reduces the ability for the heat to dissipate into the atmosphere and causes the surface to remain warmer for a longer period of time (Ng and Ren, 2012). The building heights and density of buildings restrict air flow and ventilation, which affect the ability for wind to transport warm air away and allow cooler air to flow into the area.

The building footprint layer is derived from the 2017 LARIAC dataset, which contains a height field and area field in feet and square feet, respectively. The two fields represent the height and the floor area of a given building footprint. Multiplying the values in the two fields together will result in the building volume, given in cubic feet. The resulting building volumes is then converted to cubic meters, to match the units used in Ng and Ren (2012). In the Hong Kong urban climatic map, building volume percentages were calculated and used for classification in

the following steps. This is done by dividing a given building volume value with the highest building volume value found in the entire city of Los Angeles and converted to a percentage value.

The building footprint layer excludes areas with impervious surfaces. It is necessary to include a land cover type layer to identify impervious areas which do not contain any buildings, as impervious surfaces would have a much lower thermal load impact than areas containing an urban structure. A query is used to select impervious areas and the attributes will be exported as its own separate layer. Afterwards, the impervious area layer is merged with the building footprint layer to create an output layer containing both attributes. As the selected impervious surface areas do not contain buildings, a value of zero will be assigned to the building volume and building volume percentage fields. The 'CODE' field found in the output layer will be populated with either the "Building" or "Impervious Surface" attribute, to represent the type of anthropogenic cover found at the location.

The feature polygon layer is then be converted to a raster and aggregated to a resolution of 100 square meters, based on the building volume field. Using the reclassify tool, the raster layer will then be classified based on the percentage building volume in each aggregated pixel. Areas within city boundaries and containing no building volume data are assigned a classification value of 0, while other building volume percentage values are assigned according to the classification used in Ng and Ren (2012). Pixels with a higher building volume percentage values are assigned a larger classification value, which represents a larger impact on the thermal load. Figure 3 illustrates the methodology used to build the layer, while table 2 shows the six different classifications used to classify the building volume percentage values.

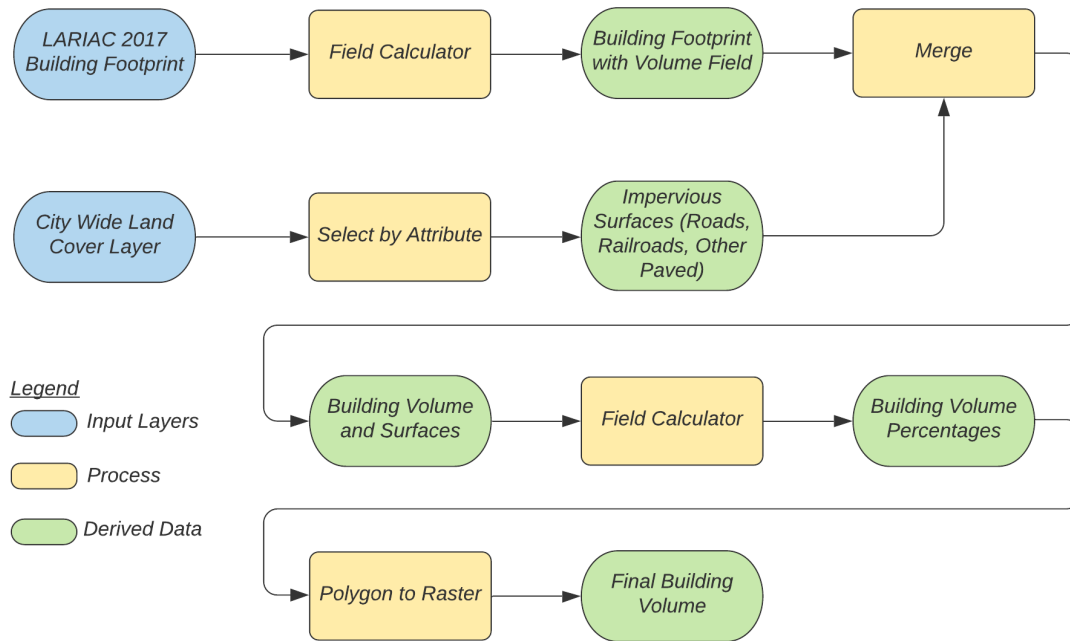


Figure 3: Building Volume Layer Methodology

Table 2: Building Volume Thermal Load Classification (Taken from Ng and Ren 2012)

Thermal Load	Building Volume Percentage (percentage range)	Classification Value
Zero	0 (no building)	0
Very Low	0 (paved areas)	1
Low	>0 – 4	2
Medium	>4 - 10	3
High	>10 - 25	4
Very High	Greater than 25	5



### 3.2.1.2. Topography

The topography of a region is crucial to developing an urban climatic map. The elevation of a region can affect the ambient temperatures of a given area, with higher elevations often much cooler than areas at lower elevations. This is due to the phenomena known as the environmental lapse rate, in which ambient air temperatures can change based on the altitude. According to a study by Golany (1996) on the climatic impacts of urban design, the ambient air temperature generally decreases by 1°C every 100m increase in elevation. Areas at lower elevations experience warmer ambient temperatures, and as a result, are more susceptible to more intense UHI effects. This is reflected in Ng and Ren (2012)'s classification, where lower elevations are assigned a higher thermal load classification value.

Using the contour layer generated from the LARIAC LIDAR dataset, a digital elevation model is created to represent the elevation for the city of Los Angeles. The digital elevation model has a spatial resolution of 100 square meters, to match the resolution of the other layers of the urban climatic map. As the original LARIAC dataset's units are in feet, the elevation values are converted to meters, to match the units used in the Hong Kong urban climatic map. The minimum classification value is adjusted to account for Wilmington, Los Angeles, with a small section of the city lying a few meters below sea level. Figure 4 illustrates the methodology for the elevation layer, and table 3 shows the classification scheme used for the topography layer.

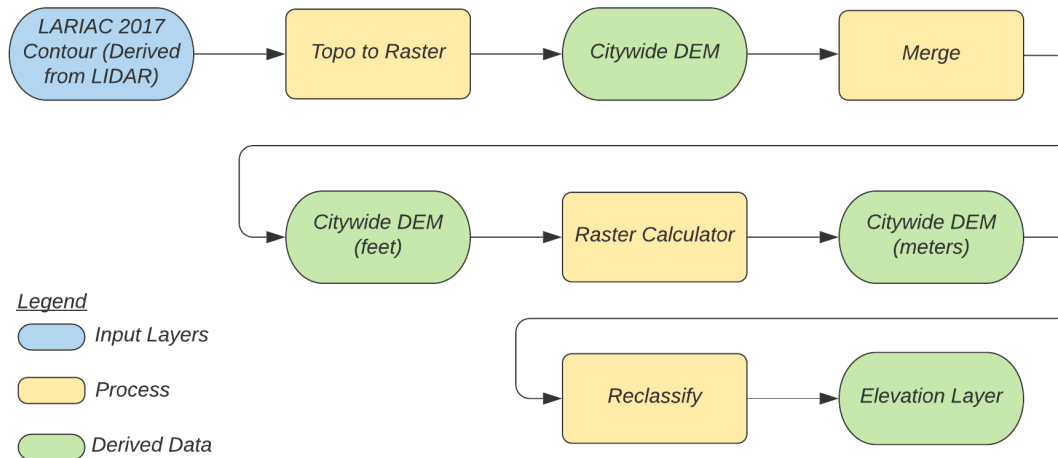


Figure 4: Elevation Layer Methodology

Table 3: Elevation Thermal Load Classification (Taken from Ng and Ren 2012)

Thermal Load	Elevation (in meters)	Classification Value
High	>-10 - 50	0
Medium	>50 - 100	-1
Low	>100 – 200	-2
Very Low	>200	-3

### 3.2.1.3. Vegetation

The third and final variable in the thermal load aspect is the vegetative cover layer. This layer describes the amount of vegetative cover found in a location. Vegetation has a cooling effect in urban areas and is often used by cities to reduce the urban heat generated by urban structures. Through evapotranspiration, plants can absorb solar radiation and cool the temperatures of heavily urbanized areas.

The vegetation of Los Angeles can be detected by calculating the NDVI using the LARIAC orthoimagery. The LARIAC Orthoimagery contains four bands: Red, Green, Blue, and Near-Infrared, two of which are used to calculate the NDVI. The equation for NDVI is given below.

$$(1) \quad \text{NDVI} = \frac{(\text{NIR} - \text{Red})}{(\text{NIR} + \text{Red})}$$

The results of the NDVI is on a scale between negative and positive one, where values close to negative one indicate anthropogenic or bare ground cover, and values close to one indicate dense vegetation. Once the NDVI values are calculated, the pixels will be aggregated to a spatial resolution of 100 square meters and reclassified. NDVI values above 0.1 will be classified as vegetative cover and values below 0.1 will be classified as non-vegetated cover. Figure 5 illustrates the methodology to build the vegetation layer, and table 4 shows the NDVI values and the impact of the vegetation on thermal load in urban areas.

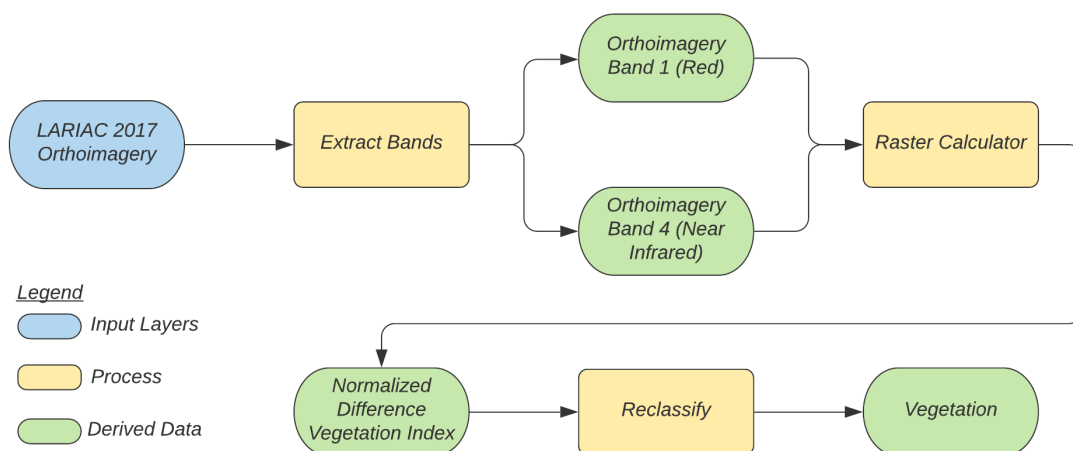


Figure 5: Vegetation Layer Methodology

Table 4: Vegetation Thermal Load Classification (Taken from Ng and Ren 2012)

Thermal Load	NDVI Values	Classification Value
Negative (Cooling)	Greater than or equal to 0.1	-1
Neutral	Less than 0.1	0

### 3.2.2. Dynamic Potential Map:

The dynamic potential aspect analyzes the urban surfaces and features that affect the wind through urbanized areas. The movement of air and the ability to ventilate air in an urban setting are crucial when analyzing the ability for the urban area to allow wind to transport heat away from the urbanized areas. The dynamic potential for Los Angeles will be composed of three layers, which describe ground coverage, natural landscapes, and proximity to openness, as defined by Ng and Ren (2012).

#### 3.2.2.1. Ground Coverage

Similar to the effect on thermal load, tall buildings have a positive effect on urban warming as they obstruct wind and air movement. This reduces the ability for the wind to transport warmer air away from urban centers and prevents cooler air to flow in from open spaces. The poor air ventilation creates a positive feedback loop, as the weaker air ventilation is not strong enough to reverse the warming effects within the urbanized area (Tsang *et al.*, 2012). The study by Tsang *et al.* (2012) analyzed the effects of the shapes of the buildings, which can reduce air ventilation in areas between such buildings using a wind model. While the building density in Los Angeles is not as high as in other major cities, such as New York or Hong Kong, there are pockets of dense urban development which can affect the area's dynamic potential.

The ground coverage layer is derived from the 2017 LARIAC building footprint layer. Using the merged layer created during the building footprint layer, a new field is created in the building footprint layer and populated with a value of one, to indicate the presence of a building or impervious surface at that location. The building footprints layer is converted to a raster based on the cover field, with a spatial resolution of one square meter. The raster is then aggregated into 100 square meter pixels, with the aggregated pixel value taking the average of the one square meter pixels. These aggregated pixel values serve as the ground coverage percentage values. Following Ng and Ren (2012)'s classification scheme, classification values are assigned according to the dynamic potential and the ability for air to move through the urban area. Figure 6 illustrates the methodology for the ground coverage layer, and table 5 shows the three classes for ground coverage.

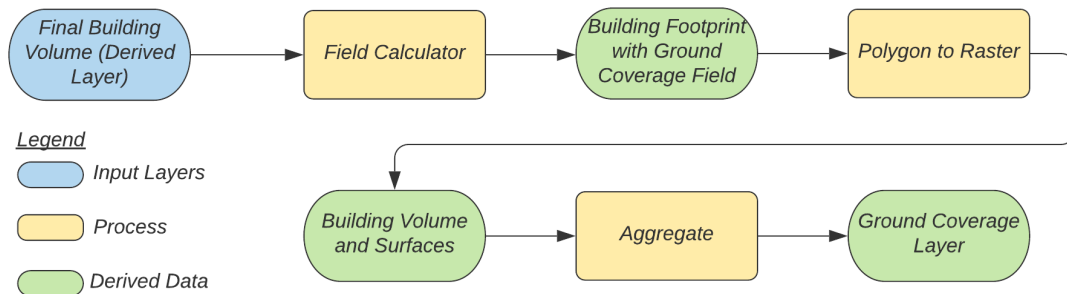


Figure 6: Ground Coverage Layer Methodology

Table 5: Ground Coverage Dynamic Potential Classification (From Ng and Ren 2012)

Air Ventilation Potential	Ground Coverage (in percent)	Classification Value
High	0 – 30	-2
Medium	>30 – 50	-1
Low	>50	0

### 3.2.2.2. Natural Landscapes

Natural landscapes, as defined in Ng and Ren (2012), describe vegetative cover which can alter the air flow and wind patterns with the city. Oke (1988) has analyzed and listed the aerodynamic properties of various features found within an urban environment, including trees. Depending on the size in a forest environment, trees have a surface roughness similar to buildings, and have the ability to restrict air flow. The Ng and Ren study calibrated the green space raster to assign a positive classification value to trees to describe the lower dynamic potential that trees have.

Identifying the trees is a similar process to identifying the vegetative cover in the thermal load section. However, the difference is that the threshold value is much higher to distinguish trees from other types of vegetation, such as grass and shrubs. Values above the threshold will be reassigned a value of one, while values below the threshold will be assigned a value of zero. This describes the reduced dynamic potential that trees have, with its ability to restrict airflow in a given area. Finally, the pixels will be aggregated to the 100 square meter resolution to make it consistent with the other layers for the urban climatic map. Figure 7 shows the methodology for the natural landscape layer, and table 6 shows the classification for the green space dynamic potential as defined in Ng and Ren (2012).

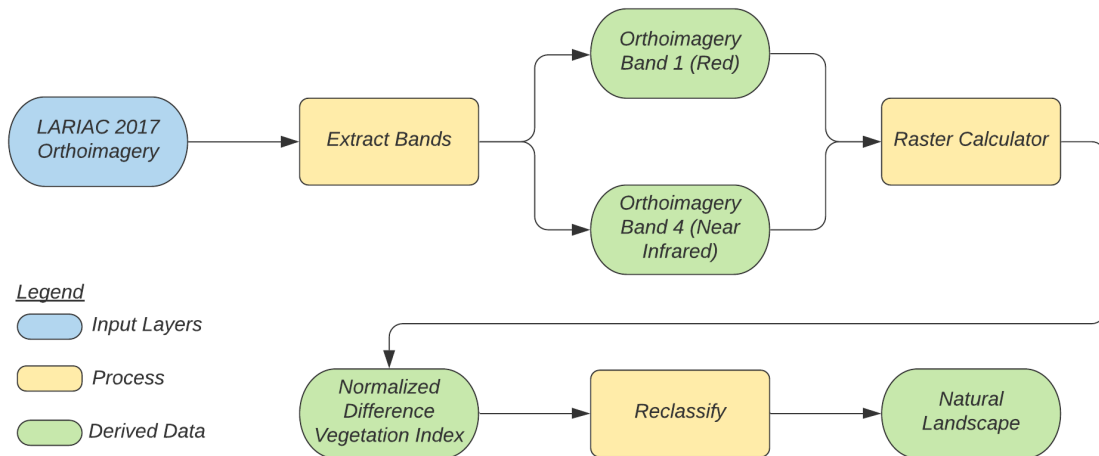


Figure 7: Natural Landscape Layer Methodology

Table 6: Green Space Dynamic Potential Classification (Taken from Ng and Ren 2012)

Dynamic Potential	NDVI Values	Classification Value
Low	Greater than or equal to 0.6	1
High	Less than 0.6	0

### 3.2.2.3. Proximity to Openness

The final component of the dynamic potential aspect is the proximity to openness. Open spaces are typically the source of cool air that blows through urbanized areas to ventilate the area. This is due to lack of urban features which obstruct air flow and allow open spaces to maintain cooler temperatures than developed urban areas. This layer is composed of three different proximity calculations: distances measured from the coastline, an open space/park within the city, and slope, which has the potential to increase the movement of air and the cooling effect in the city.

The first open space layer calculates the distance away from the coastline, where the sea is a source of cooler air that has the potential to ventilate urban areas. Buffering the coastline data multiple times at various distances is done to visualize the diminishing cooling effect sea breezes have as it moves inland. Ng and Ren (2012) has set the buffering values at 70 meters and 140 meters away from the coastline. Once the buffers are created, a field is added to the layer, and a classification value is assigned to this field based on the distance the point is from the coastline. In addition to the coastline proximity buffer, ground coverage is also considered when determining the dynamic potential of the buffered regions. The final layer is a raster layer aggregated to 100 square meters to match the spatial resolution of the urban climatic map. The methodology for this layer is visualized as a flowchart in figure 8, while table 7 shows the different dynamic potential values based on the different distances from the coastline.

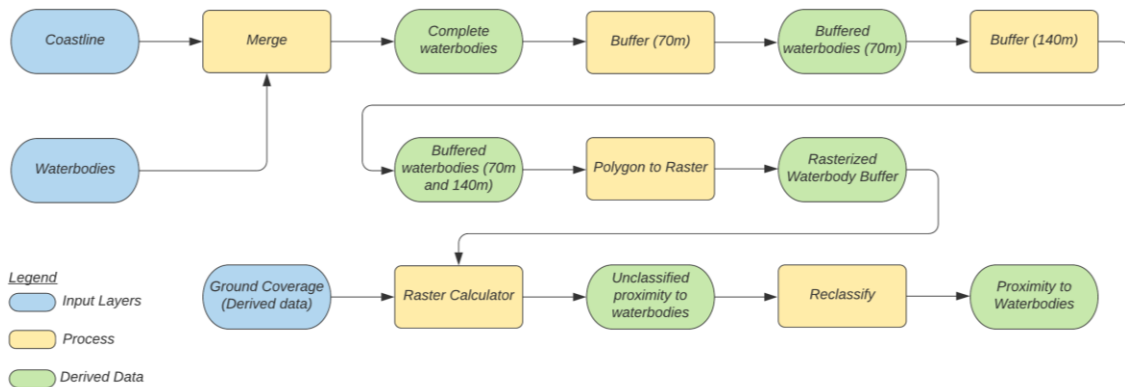


Figure 8: Proximity to Waterbodies Layer Methodology



Table 7: Distance from Coastline Dynamic Potential Classification (From Ng and Ren 2012)

Dynamic Potential	Distance from Coastline (in feet)	Classification Value
High	Close to coastline (0-70m) and low ground coverage (<30%)	-2
Medium	Close to coastline (0-70m) with medium ground coverage (30-50%) <b>or</b> medium distance from coastline (70-140m) with low ground coverage (<30%)	-1
Low	Far from coastline (>140m) <b>or</b> high ground coverage (>50%) <b>or</b> medium distance from coastline (70-140m) with medium ground coverage (30-50%)	0

The second open space layer calculates the distance away from the open spaces within the city, such as parks. The parks data can be obtained from the parks dataset, while the open spaces can be obtained from the general plan land use layer from the Los Angeles Department of City Planning. A buffer of 100 meters around the parks and open spaces found within the city is done to simulate the movement of cooler air from open spaces into the built environment. The open space areas and the buffered areas are then merged and converted to a raster, with each pixel covering an area of 100 square meters. Identified pixels containing parks and open spaces are assigned a classification value of -1. The methodology is visualized in figure 9, and table 8 shows the open space dynamic potential classifications.

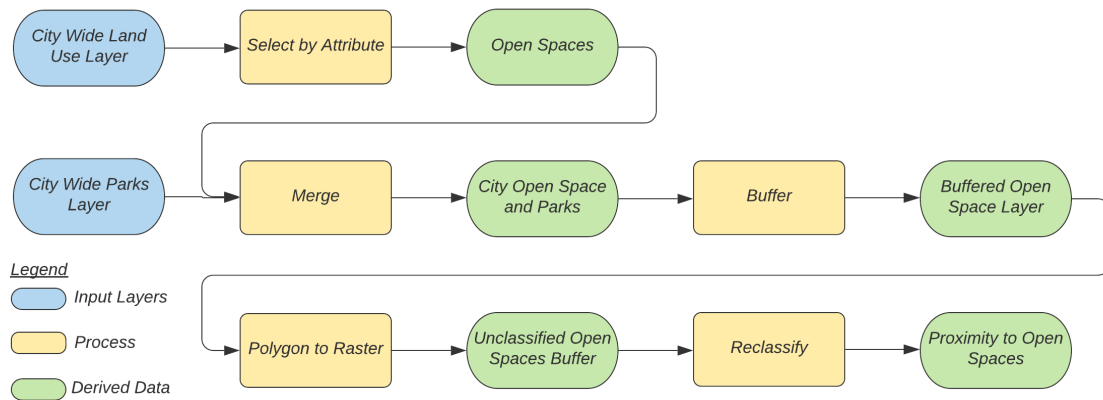


Figure 9: Proximity to Open Spaces Layer Methodology

Table 8: Open Space Dynamic Potential Classification (Taken from Ng and Ren 2012)

Raster Benefits from Open Space	Classification Value
Yes	-1
No	0

The final component in the open space layer is the slope from the digital elevation model. In normal circumstances, steep vegetated terrain has the potential to increase wind velocity. The Santa Ana winds in Southern California are a type of wind event that moves air from the Great Basin towards the southern California region. The surrounding mountain range, the Transverse Range, funnels the wind through the canyons, increasing the wind velocity and the dynamic potential to ventilate urban areas. As a result, canyons with steeper slopes will have a higher dynamic potential for air ventilation, which will produce a cooling effect on urban heat, regardless of temperature.

Using the digital elevation model, the slope is calculated and aggregated to 100 square meter pixels. Pixels with a slope of 40% or more are classified with a value of -1 and used as a threshold value to determine whether the area the raster covers is benefiting from the dynamic potential of the slopes. The vegetation layer is used in conjunction with the slope layer to identify vegetated slopes. If there is vegetated cover overlaid on the pixels classified with a slope greater than 40%, then the classification value of -1 will be kept. Otherwise, the pixel's classification value will be changed to zero. The methodology is illustrated in figure 10, and table 9 shows the dynamic potential classification for slopes.

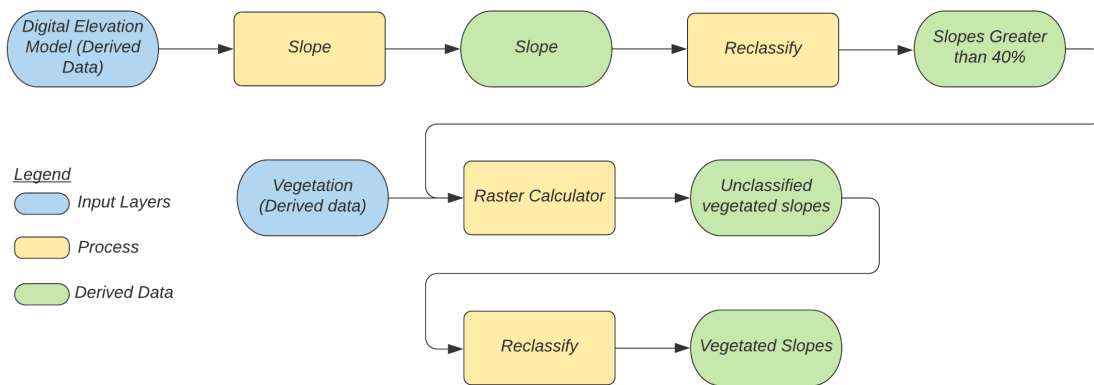


Figure 10: Proximity to Open Spaces Layer Methodology

Table 9: Slope Dynamic Potential Classification (Taken from Ng and Ren 2012)

Vegetated slopes of 40% and above	Classification Value
Yes	-1
No	0

### 3.2.3. Wind Data

Wind data is a highly complex variable and is difficult to accurately model in an urban climatic map. However, throughout its existence, researchers have taken many different approaches to model the necessary wind data and incorporate wind information into the urban climatic map. In early urban climatic maps, German researchers utilized wind roses to identify the prevailing wind conditions and air ventilation zones within the city (Baumüller *et al.* 1992). As a result, later urban climatic map studies have used the wind rose to visualize the key wind patterns within the study area, using the early methodologies as a standard. Ng and Ren (2012) built upon this work to model an accurate wind environment for Hong Kong. Using a combination of weather station datasets and the MM5 mesoscale meteorological model, Ng and Ren (2012) predicted prevailing wind conditions and identified air ventilation zones within the city.

For the Los Angeles urban climatic map, the wind dataset is taken from the National Oceanic and Atmospheric (NOAA) National Centers for Environmental Information (NCEI). NOAA has various weather stations located around Los Angeles, usually at airfields or large open spaces where environmental factors such as people or tall buildings would not have a significant impact on the temperature reading. The dataset contains hourly, daily, and monthly averages for climate information, such as temperature, precipitation, humidity, air pressure, and wind speed and direction.

Due to the different wind conditions that are present in the Los Angeles area, it is necessary to distinguish between each of these wind conditions for the urban climatic map. Prevailing winds, sea breezes, and seasonal wind conditions, such as the Santa Ana winds are analyzed to understand wind patterns that affect the urban climate. The NCEI dataset is divided into two datasets, one analyzing wind data for the months of June to August, and the second

analyzing wind data for the months of October to January. This is done to capture the wind data under normal summer season conditions when the UHI is strongest, and the seasonal Santa Ana wind conditions. Table 10 identifies the weather stations and their locations where the wind speed and wind direction data are collected for the Los Angeles urban climatic map.

Table 10: NOAA NCEI Weather Stations

Name/Location	Station ID	Latitude	Longitude
Burbank-Glendale-Pasadena Airport	WBAN:23152	34.20056	-118.3575
Hawthorne Municipal Airport	WBAN:03167	33.92278	-118.33417
Long Beach Airport	WBAN:23129	33.8116	-118.1463
Los Angeles Downtown, USC	WBAN:93134	34.0236	-118.2911
Los Angeles International Airport	WBAN:23174	33.938	-118.3888
Los Angeles Whiteman Airport	WBAN:53130	34.25917	-118.41333
San Gabriel Valley Airport	WBAN:03165	34.08333	-118.03333
Santa Monica Municipal Airport	WBAN:93197	34.01583	-118.45139
Van Nuys Airport	WBAN:23130	34.20972	-118.48917
Zamperini Field	WBAN:03174	33.80338	-118.33961

Wind roses are constructed to average the hourly wind information dataset gathered from the weather stations under the NCEI program and visualize the prevailing wind conditions for the month. A Python script is used to parse the wind data for each weather station and will output a wind rose summarizing the prevailing wind conditions during the summer months and the Santa Ana wind months. Using the wind roses, wind arrows representing the prevailing wind conditions are added as two separate maps, one to show the wind conditions during summer months and the other map showing wind conditions during the Santa Ana wind months. Figure 11 shows the Python script used to generate the wind roses, and figure 12 shows the wind rose based on data from the summer months of 2017 recorded at USC.

```
1  from windrose import WindroseAxes
2  import matplotlib.pyplot as plt
3  import numpy as np
4  import pandas as pd
5
6
7  test = pd.read_csv('DTLA_USC.csv', error_bad_lines=False, delimiter=";")
8  wd = test['HourlyWindDirection']
9  ws = test['HourlyWindSpeed']
10 print(wd, ws)
11
12
13 ax = WindroseAxes.from_ax()
14 ax.bar(wd,ws,normed=True)
15 ax.set_yticks(np.arange(10, 60, step=10))
16 ax.set_yticklabels(np.arange(10, 60, step=10))
17 #ax.set_title('Downtown Los Angeles, USC Campus (Summer 2017)')
18 ax.legend(title="Wind Speed (MPH)", loc='upper center', bbox_to_anchor=(0.5, -0.05),
19           fancybox=True, shadow=True, ncol=5)
20 plt.savefig('DTLA_USC.png', transparent=True)
21
```

Figure 11: Example Wind Rose Python script

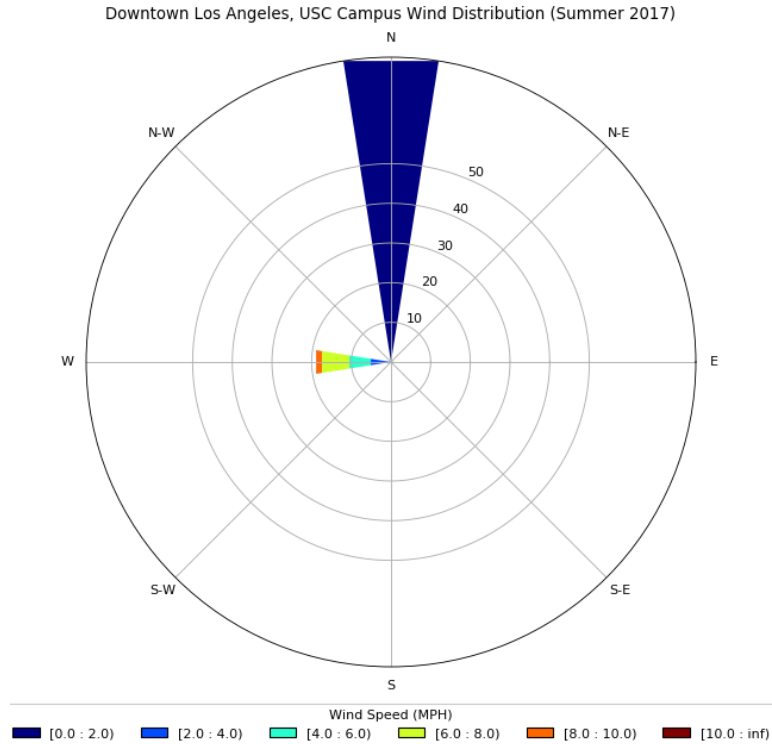


Figure 12: Summer 2017 USC Wind Rose in miles per hour

### 3.2.4. Urban Climatic Map

The final urban climatic map is created by overlaying the classified raster layers together, while also including the wind arrows created from the wind data. Using the raster calculator tool, the thermal load map and the dynamic potential map are created by adding the six classified raster layers together. The thermal load map is the sum of the building volume, topography, and vegetation raster layers, while the dynamic potential map is the sum of the ground coverage, green space, and proximity to openness layers. Table 11 is a summary table of the urban climatic variables, what the variable represents, the variable data sources, the variable weight value ranges showing the range of values used to classify and weight each layer, and the variable's impact to the urban heat island.









Table 11: Urban Climate Variable Summary

Variable Name	Variable Description	Variable Sources	Variable Weights Value Range	UHI Impact
Building Volume	Percentage of the building volume found in the city	LARIAC Building Footprint Layer, City Wide Land Cover Layer	0, 1, 2, 3, 4, 5	Positive
Topography	Elevation of the area	LARIAC 2017 Contour Dataset	-3, -2, -1, 0	Negative
Vegetation	Areas containing vegetation	LARIAC 2017 Orthoimagery	-1, 0	Negative
Ground Coverage	Percentage of ground that is covered by an impervious surface or building	Building Volume Layer (Derived from LARIAC Building Footprint)	-2, -1, 0	Negative
Natural Landscape	Areas with clusters of trees	LARIAC 2017 Orthoimagery	0, 1	Positive
Proximity to Openness	Distance from open areas, such as the coast, parks, open spaces, and vegetated slopes	Los Angeles County Boundary Layer, City Wide Land Use Layer, Ground Coverage Data (Derived from LARIAC Building Footprint Layer), LARIAC Contour Dataset	-4, -3, -2, -1, 0	Negative



The resulting raster classes are then reclassified and grouped together to create eight urban climate classes as described in Ng and Ren (2012). These eight classes are based on the different thermal loads and dynamic potentials that is expected for the area. These urban climate classifications also describe the urban heat island potential and impacts of the area. Table 12 summarizes the eight different urban climate classification types based on the classifications for the Hong Kong urban climate map by Ng and Ren (2012), and the corresponding colors used to symbolize the classes.

Table 12: Urban Climate Classification Descriptions

Urban Climate Class	Class Symbol	Classification Name	Classification Description
1		Moderate Negative Thermal Load and Good Dynamic Potential	High elevation areas and steep vegetated slopes.
2		Some Negative Thermal Load and Good Dynamic Potential	Areas covered by natural vegetation, greenery, including hilly slopes and coastal areas.
3		Low Thermal Load and Good Dynamic Potential	Areas containing spaced out development with little ground coverage. Includes open areas within the city and sparse development in coastal areas.
4		Some Thermal Load and Some Dynamic Potential	Areas containing low to medium building volumes in an open, developed environment. These include open spaces found in between buildings.
5		Moderate Thermal Load and Some Dynamic Potential	Areas containing medium building volumes located in low elevation inland areas.
6		Moderately High Thermal Load and Low Dynamic Potential	Areas consisting of medium to high building volumes found in low elevation areas and found usually in developed areas with little green space.
7		High Thermal Load and Low Dynamic Potential	Areas containing a majority of high building volumes located in well-developed, low elevation areas.
8		Very High Thermal Load and Low Dynamic Potential	Areas containing very high and compact building volumes with very limited open areas. Very little air ventilation due to the obstruction caused by tall buildings.

### *3.2.5. Validation and Linear Regression*

Validating the results of the urban climatic map involves comparing the classification results of the urban climatic map with another map which classifies the urban heat island effect. The CalEPA's Urban Heat Island Index is used as a reference to verify the accuracy of the urban climatic map. Both the CalEPA Urban Heat Island Index and the urban climatic map describe the potential warming and cooling in a specific region. This similarity allows the Urban Heat Island Index to be grouped into the same number of categories as the urban climatic map in order to make a comparison between the two models.

A linear regression model is used to explain the relationship between the CalEPA Urban Heat Island Index and the urban climatic map for Los Angeles. However, the CalEPA model utilizes a mesoscale meteorological model, which includes wind and temperature as a key input in determining the urban heat island index, a variable that is not present in the urban climatic map. As a result, an Ordinary Least Squares (OLS) regression model is used to determine any missing variables which is missing from the urban climatic map when comparing it with the CalEPA Urban Heat Island Index model. While the CalEPA model uses temperatures based on the Degree Day units to represent the warming and cooling of a region, temperature measurements have variable effects which can differ based on region. As a result, the only significant variable that can be tested in the OLS regression model is the wind speed class variable.

## **Chapter 4 - Results**

The results chapter presents the components created for the urban climatic map as well as how they are used to build Los Angeles' urban climatic map. The chapter is organized by each of the components of the urban climatic map, the thermal load variables and the dynamic potential variables. The results are visualized through maps describing the classifications for each of the variables in the urban climatic map. Finally, the results of the linear regression model to identify the fitness of the urban climatic model with the CalEPA's urban heat island index model.

### **4.1. Thermal Load Map**

The thermal load map is a measurement of the potential heat the region can absorb. It is based on building volume, topography, and vegetation of the area. building volume variable is created from a combination of the building footprint layer and impervious attributes selected from the citywide land cover layer. Figures 13, 14, and 15 show the final building volume, topography, and vegetation layers that are used as the components to produce the thermal load map. Figure 16 is the final thermal load map which would be one of the final components for the urban climatic map.

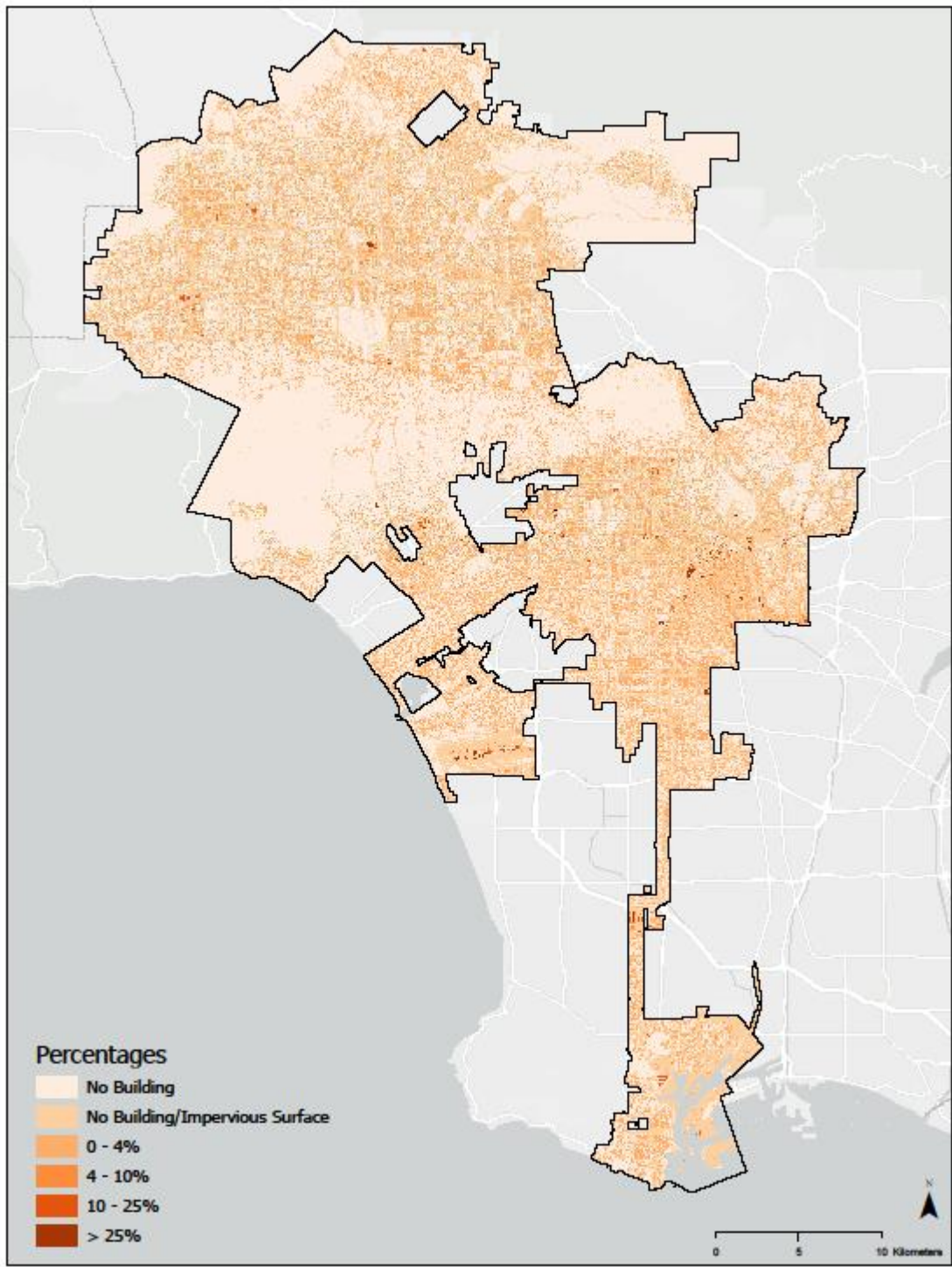


Figure 13: Building Volume

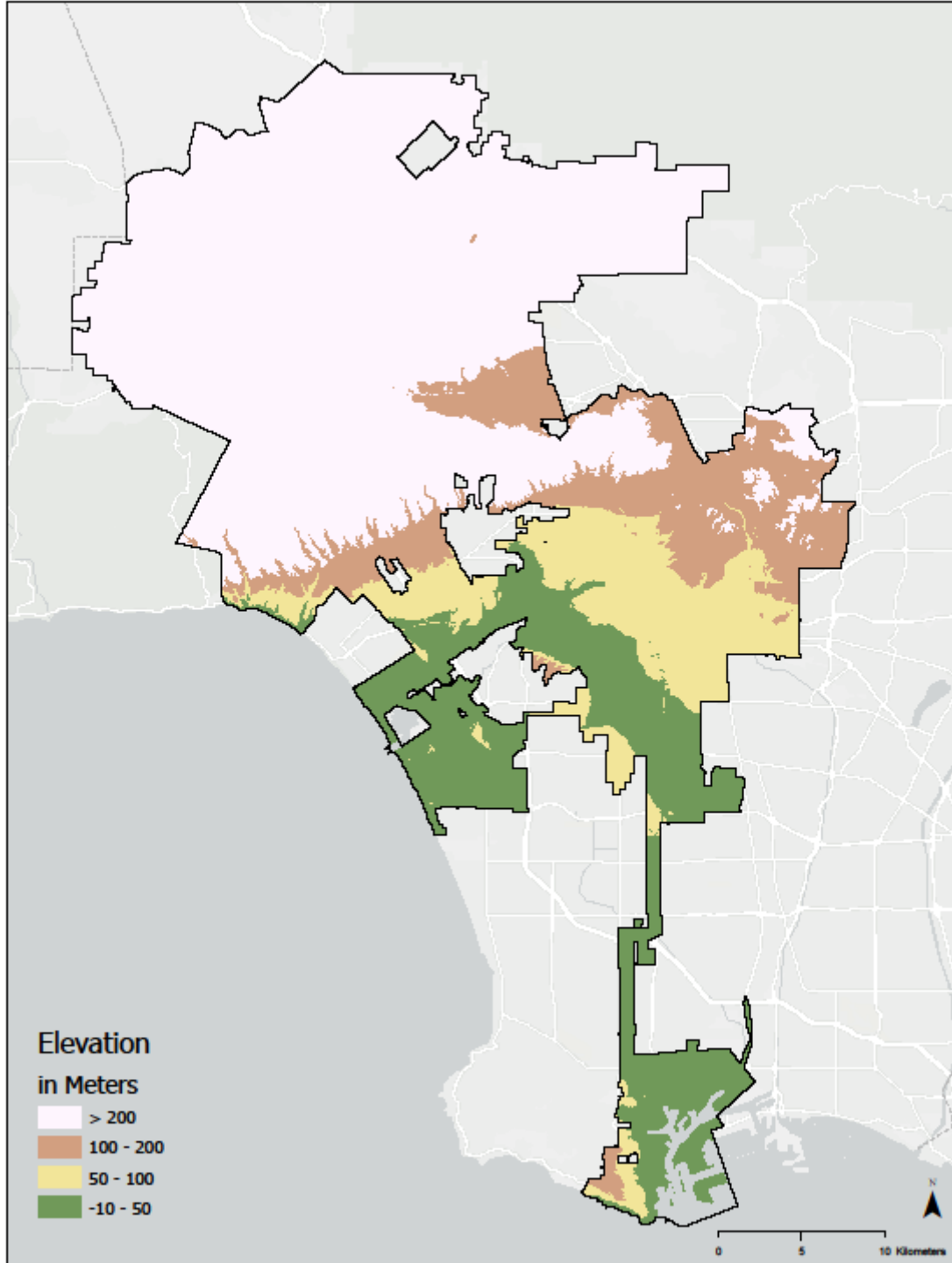


Figure 14: Topography

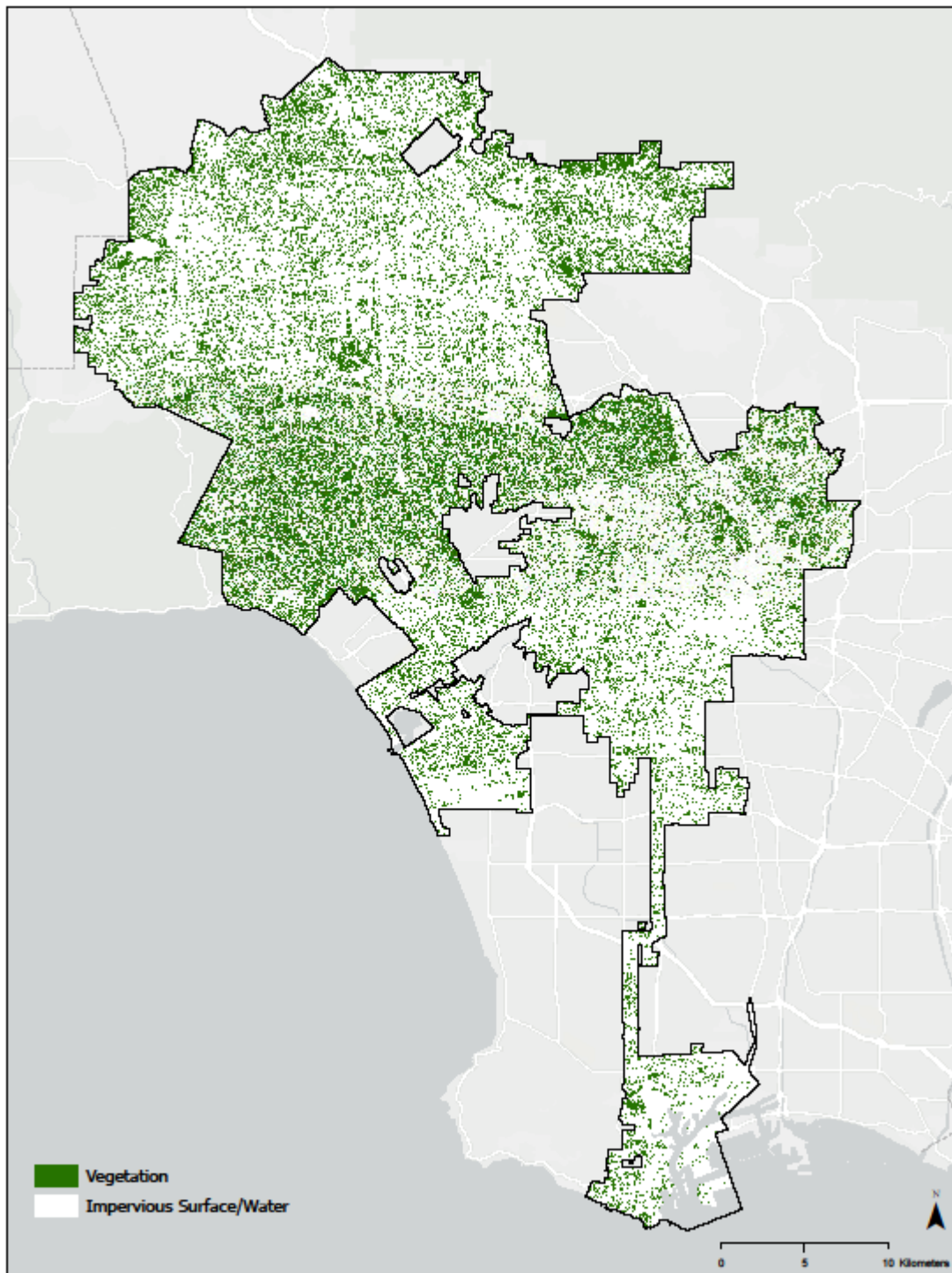


Figure 15: Vegetation

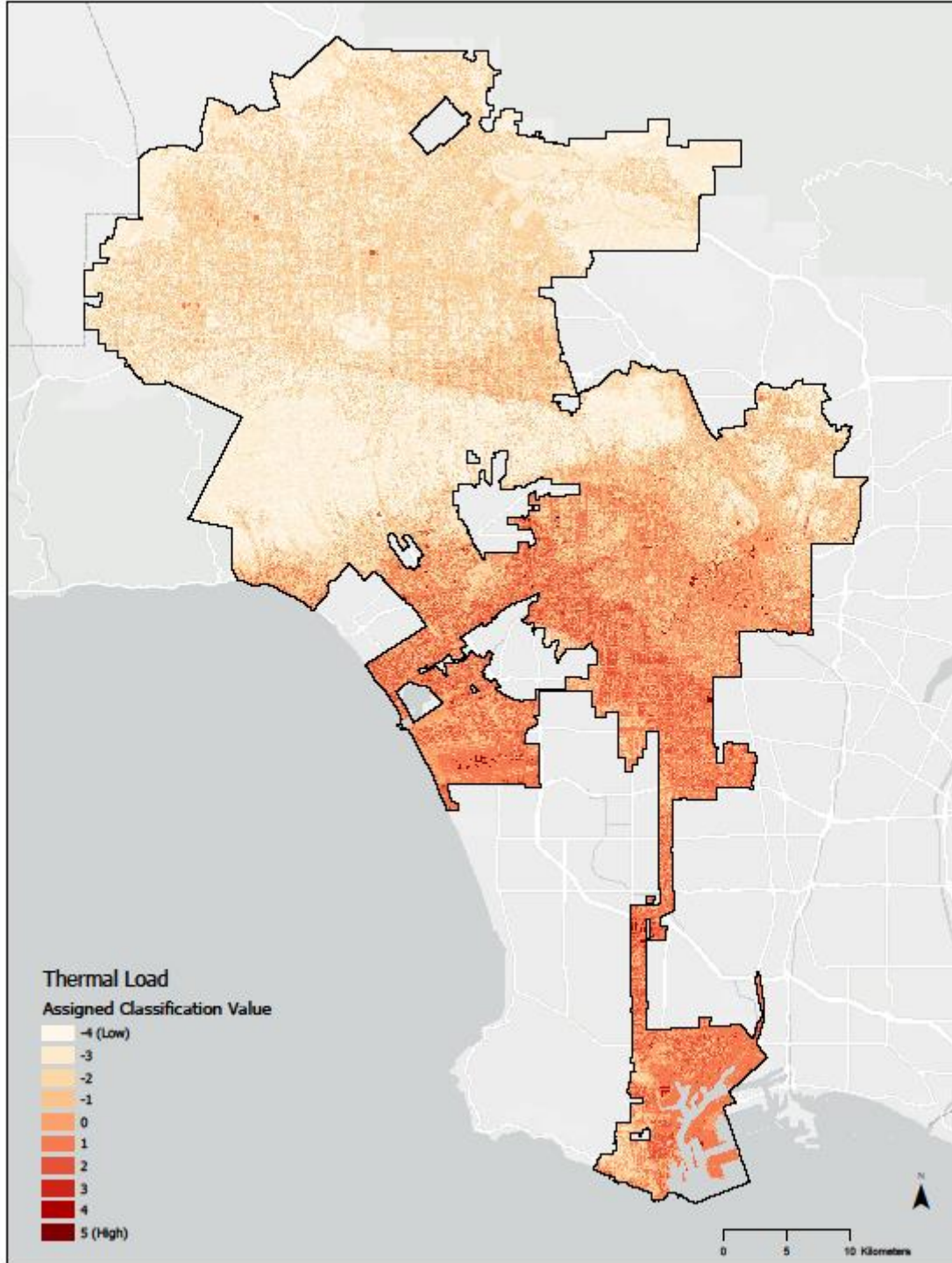


Figure 16: Thermal Load Map



## **4.2. Dynamic Potential Map**

The dynamic potential map is a representation of how well air can move throughout a region. It is based on the ground coverage, natural landscapes which impede air movement such as trees, and proximity to openness, as described in the Hong Kong urban climatic map. The ground coverage and natural landscape variables are shown in figures 17 and 18, respectively. The proximity to openness itself is composed of three other variables, which include proximity to waterfront, proximity to open spaces, and vegetated slopes. Figures 19, 20, and 21 show the components of the proximity of openness variable, shown in figure 22. Figure 23 shows the final dynamic potential map which is used as the component to build the draft urban climatic map.

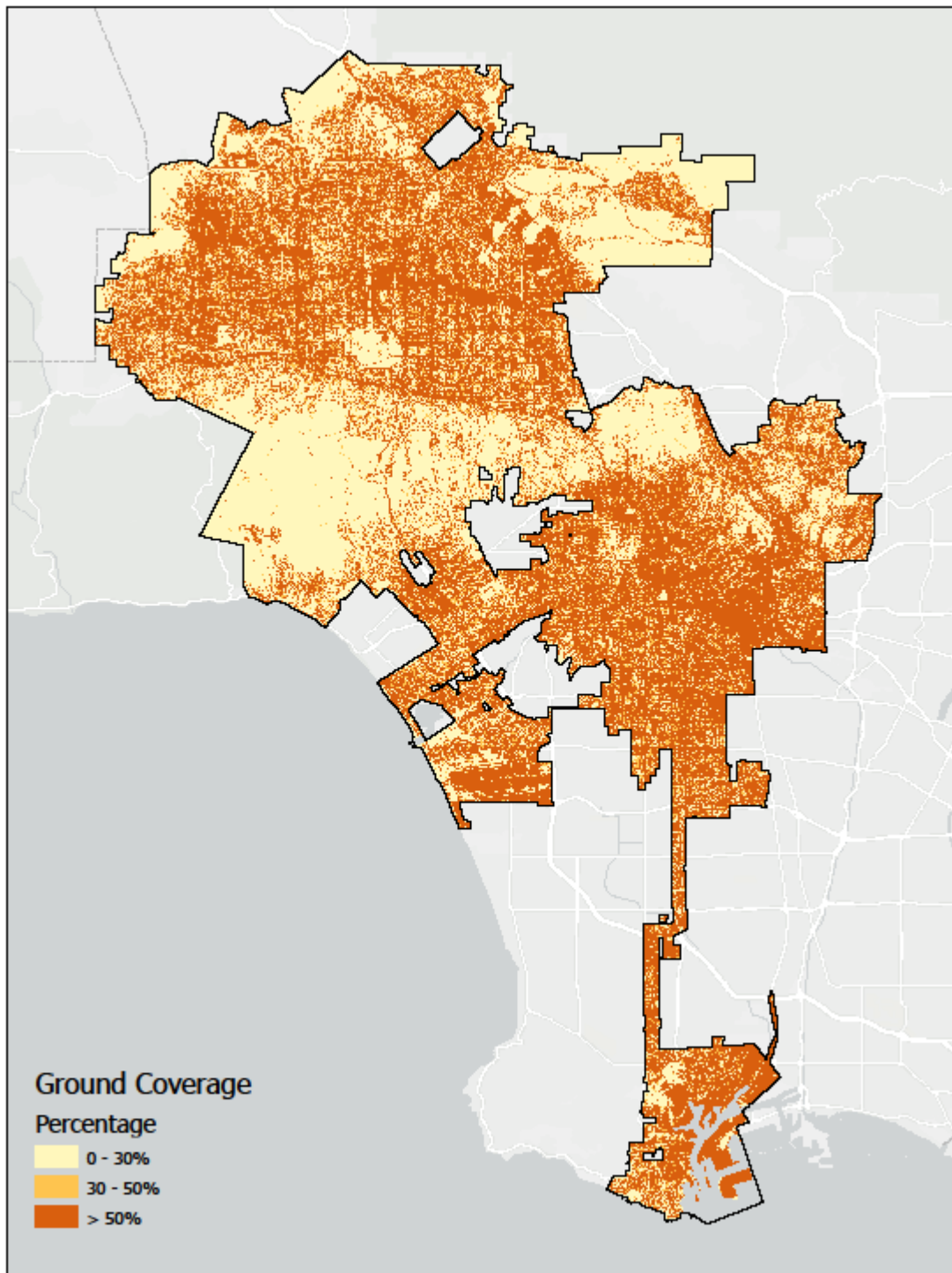


Figure 17: Ground Coverage

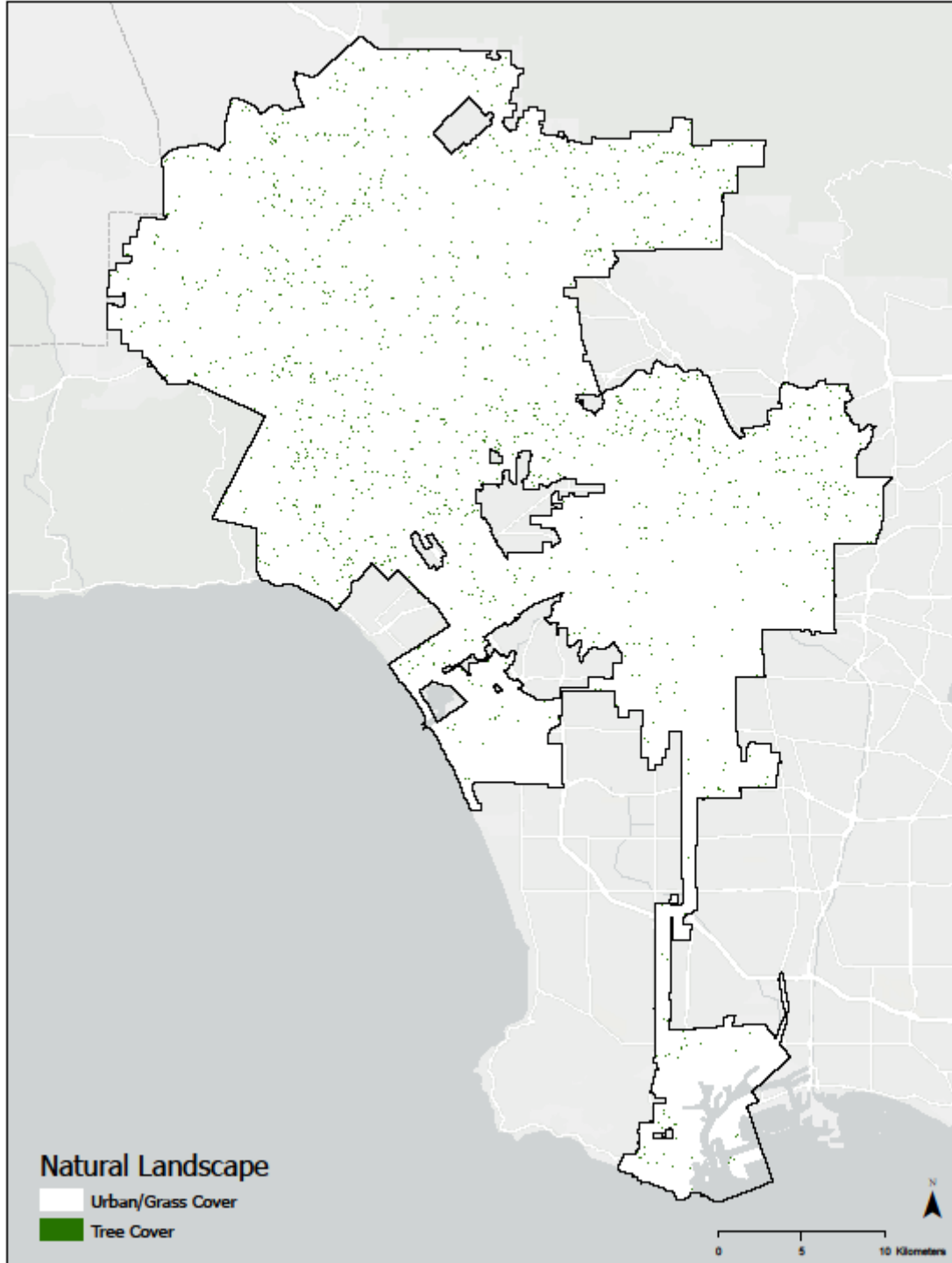


Figure 18: Natural Landscape Cover

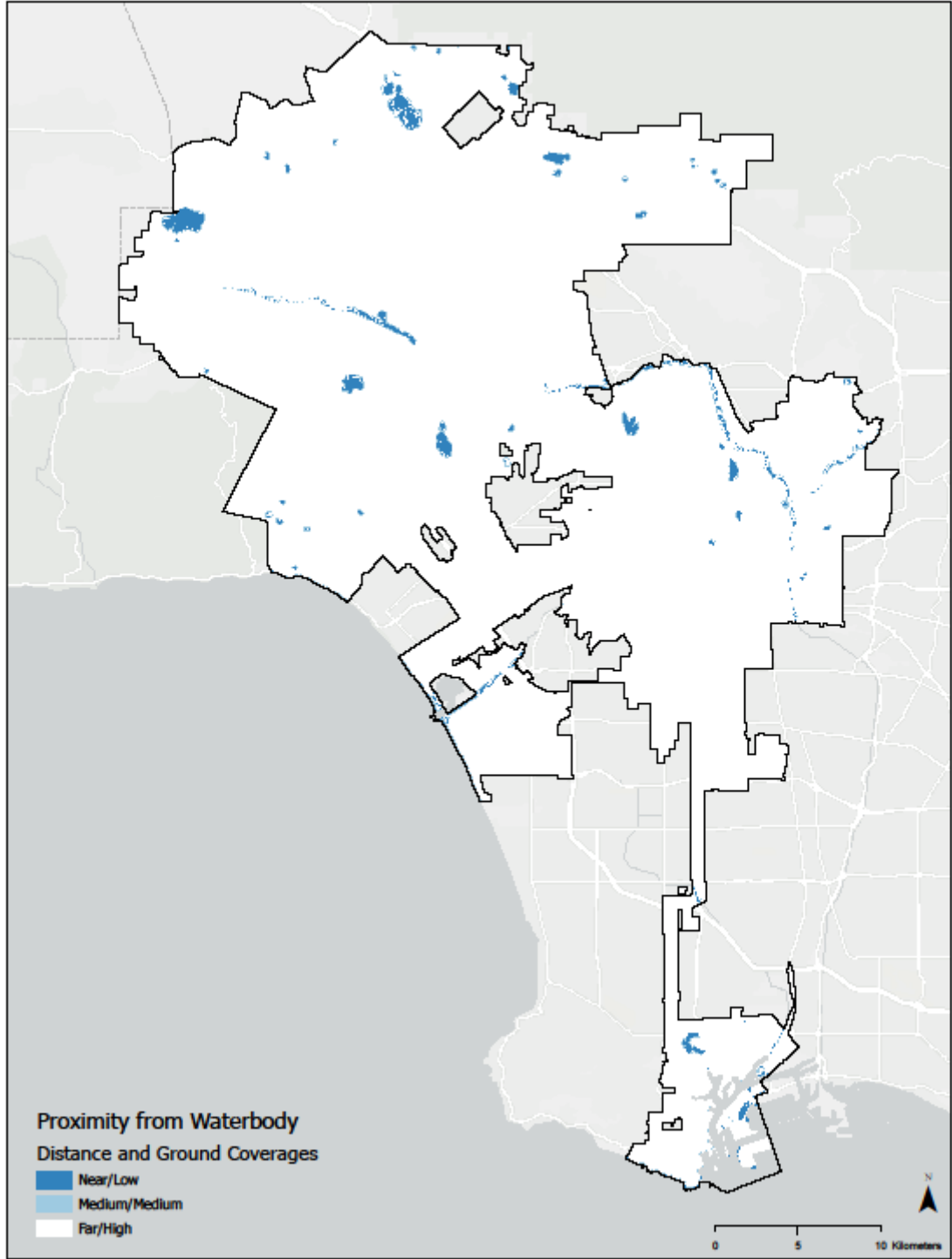


Figure 19: Proximity to Waterfront

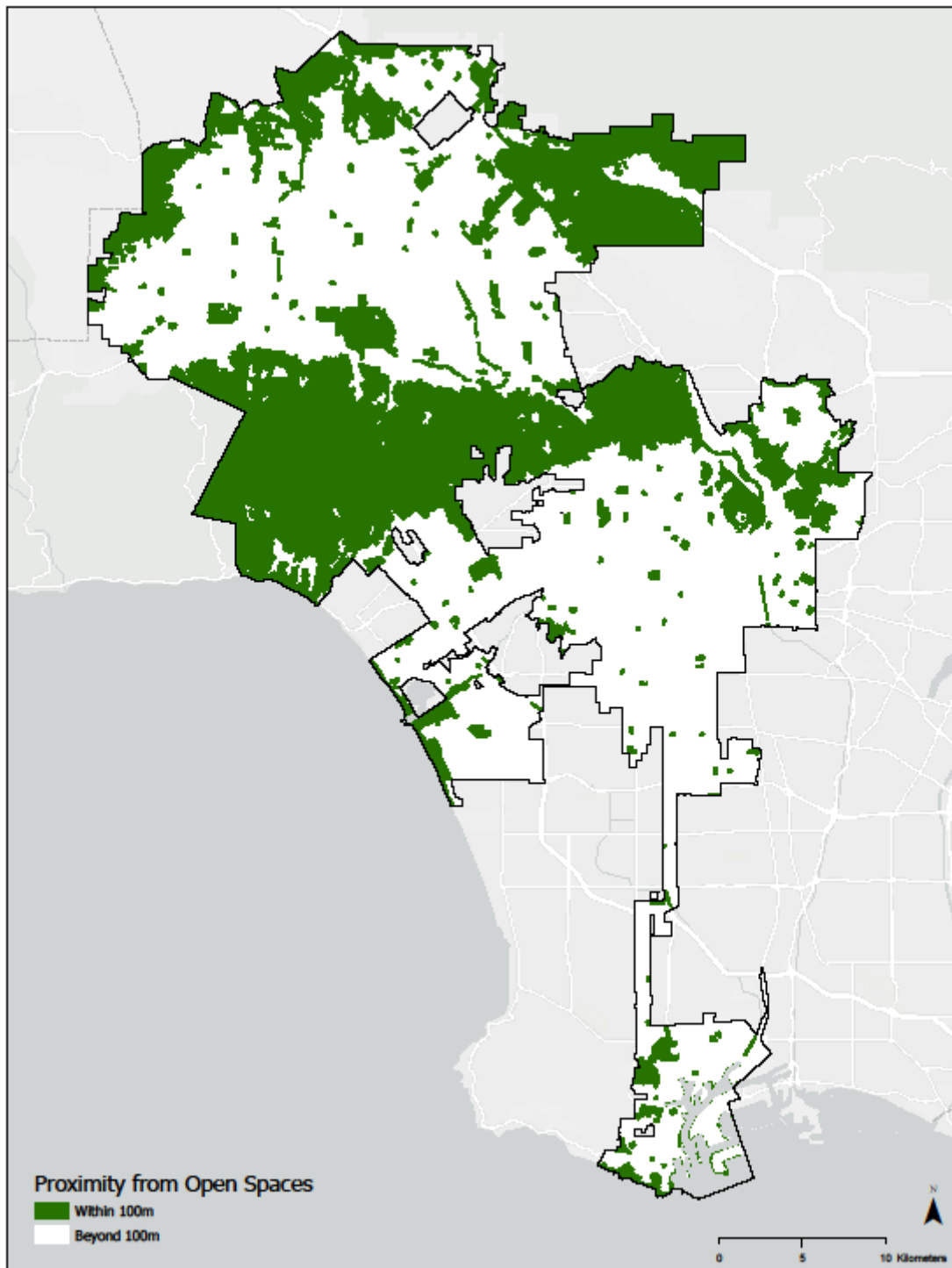


Figure 20: Proximity to Open Spaces

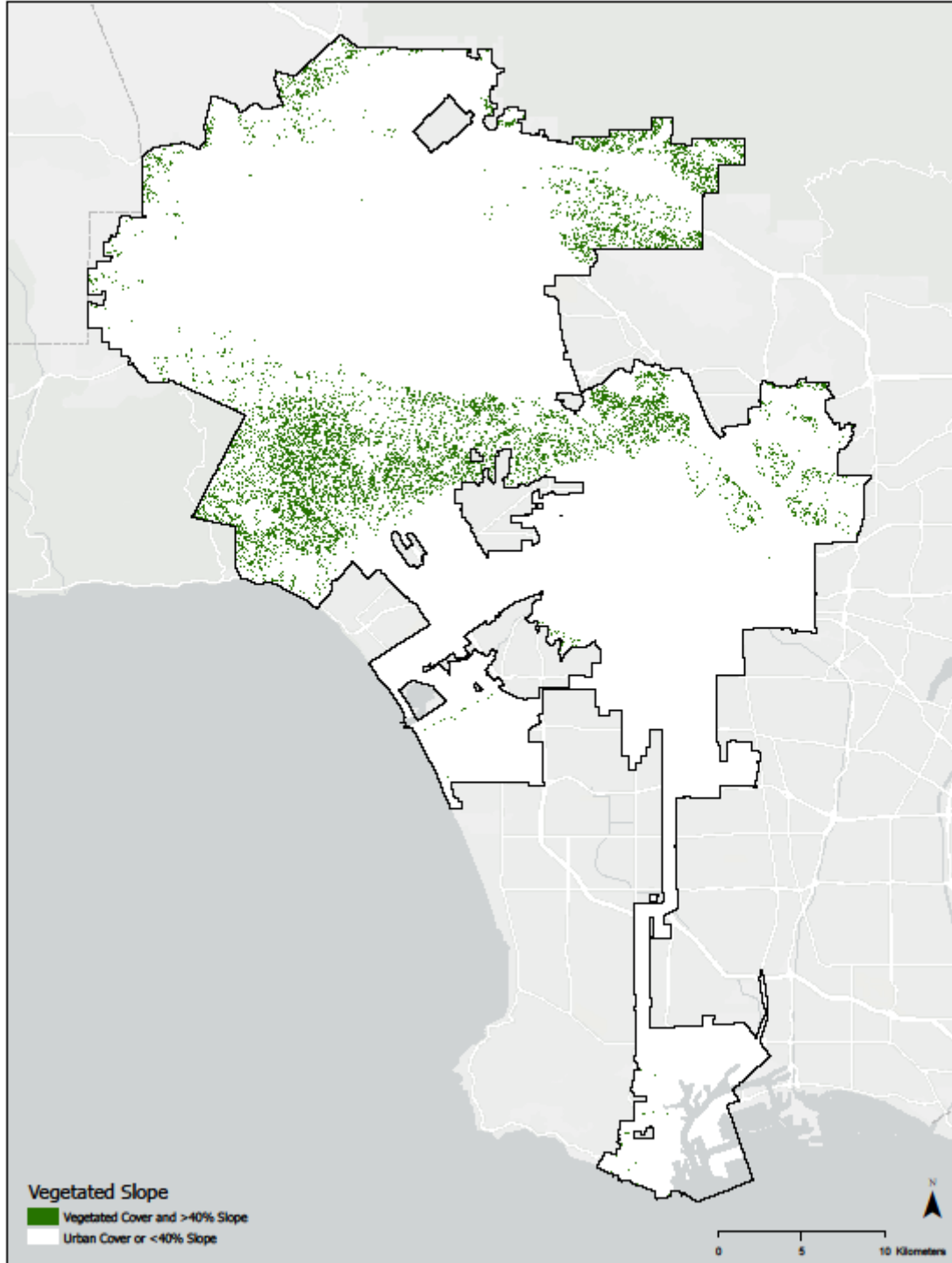


Figure 21: Vegetated Slopes

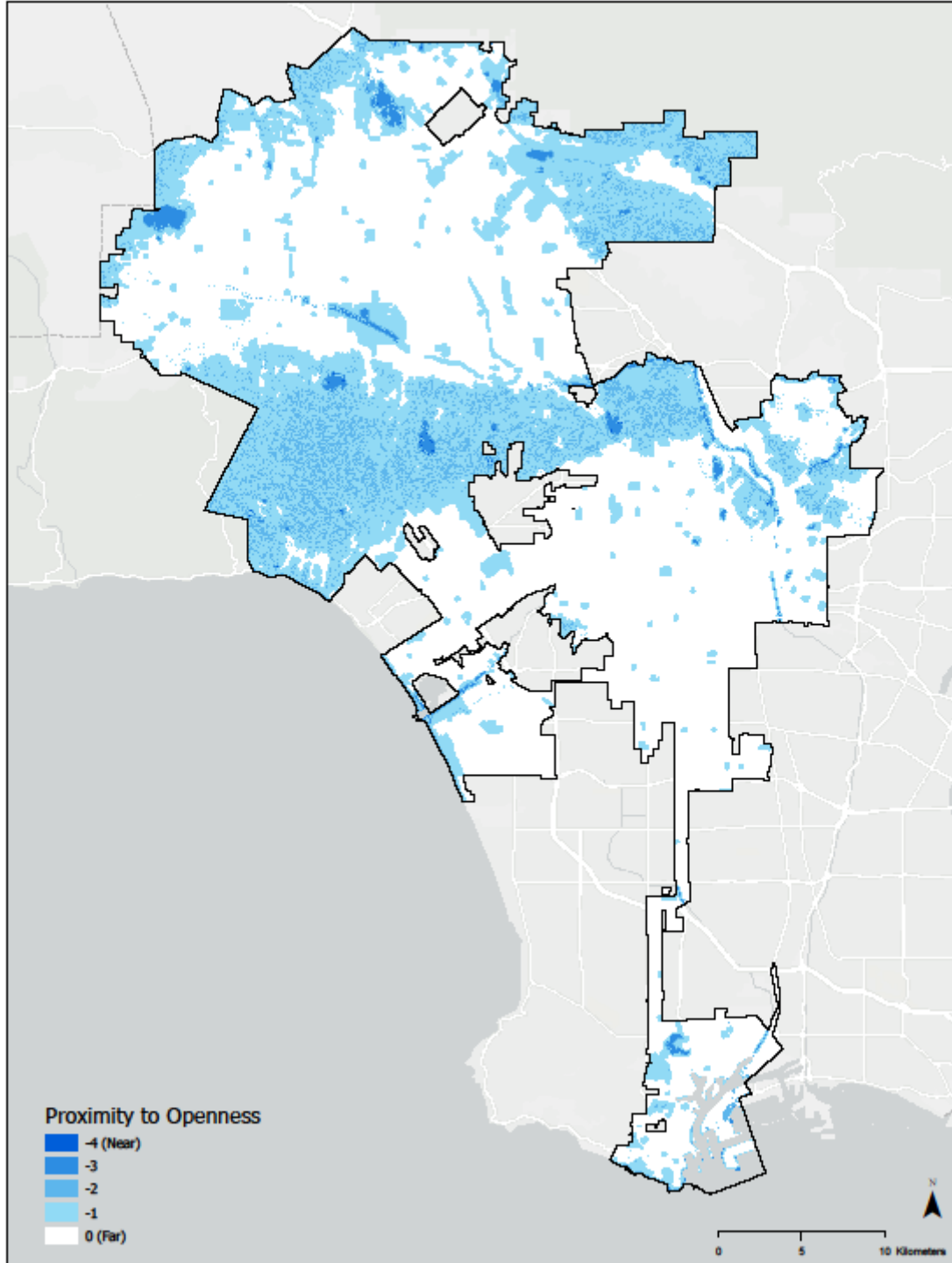


Figure 22: Proximity to Openness

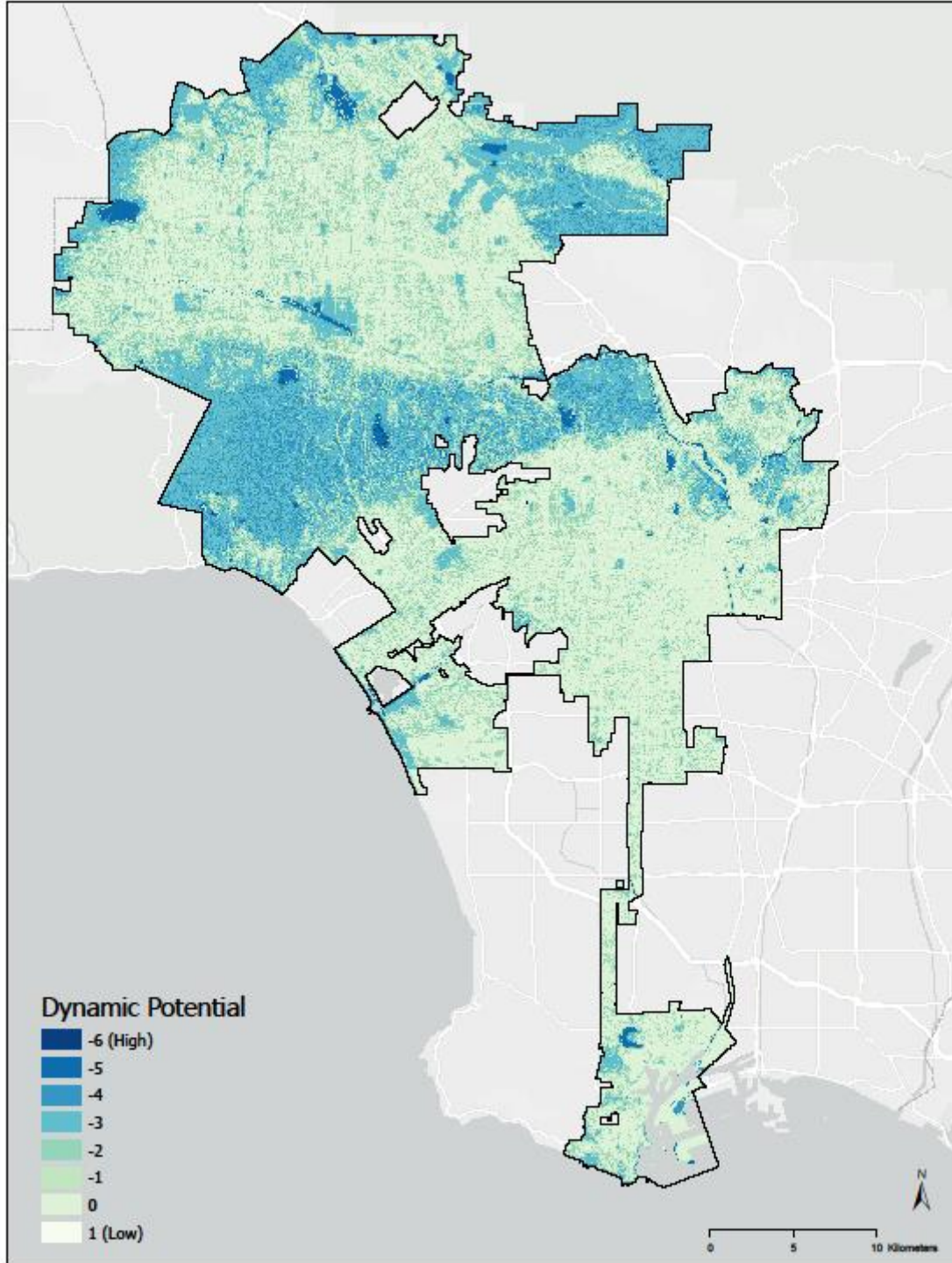


Figure 23: Dynamic Potential Map



### **4.3. Urban Climatic Map without the Wind Layer**

The draft urban climatic map is produced from combining the thermal load map and the dynamic potential map. This process creates a raster with values ranging from -10 to 5. Figure 24 shows the reclassified urban climatic map into the eight urban climate classes.

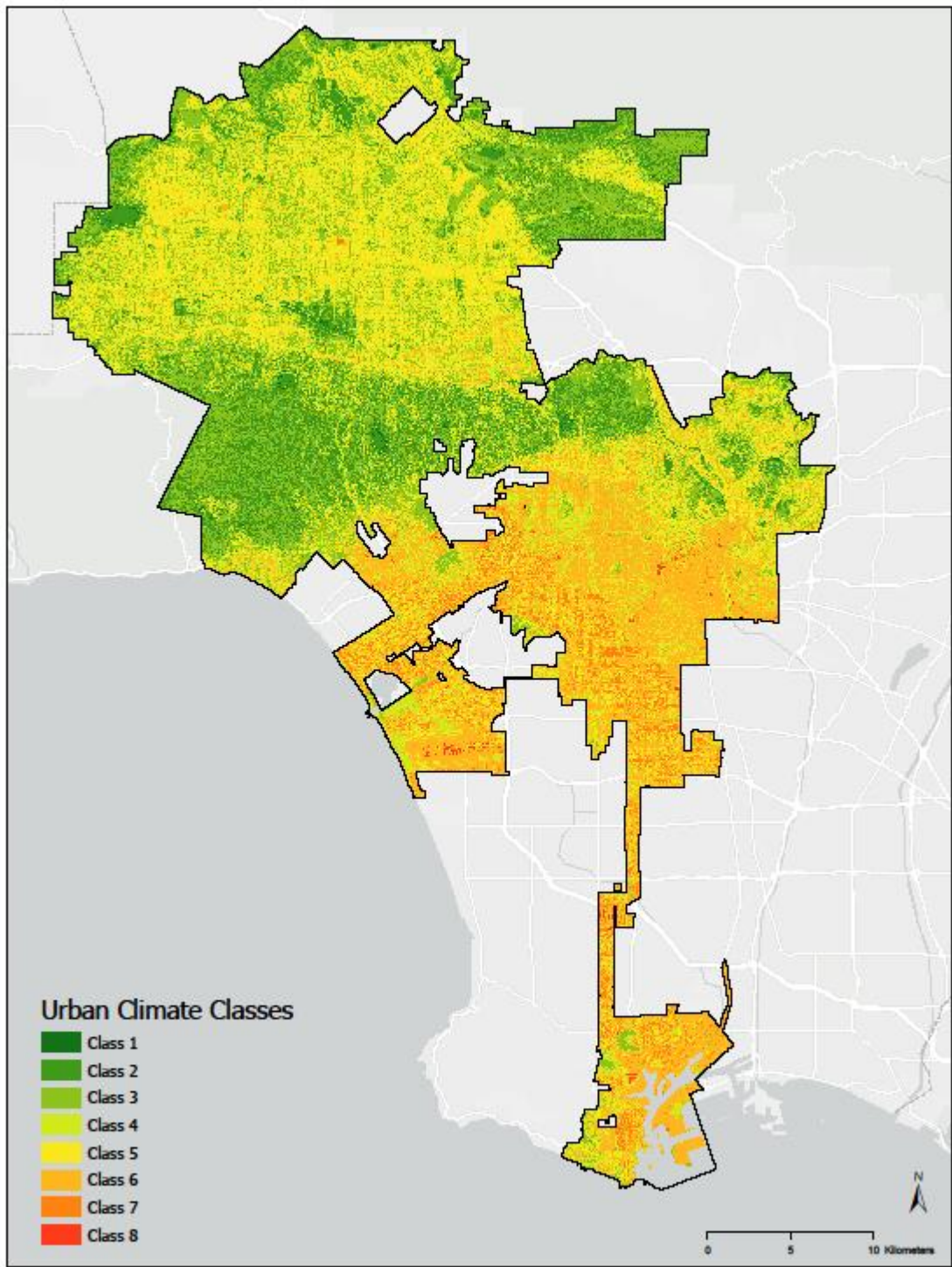


Figure 24: Draft Urban Climatic Map

#### 4.4. Validation/Regression Map

The linear regression model to compare the fitness of the urban climatic. The first Ordinary Least Squares model is used to identify the fitness of the urban climatic map classes with the degree day values by census tract from the CalEPA urban heat island index. The resulting  $R^2$  value for this model was 0.033050. The low  $R^2$  value indicates a large discrepancy between the CalEPA urban heat island index model and the urban climatic map model. Figure 25 shows the results of the Ordinary Least Squares model, with calculations representing model significance and statistical biases. The regression equation to model the best fit between the two variables is also given below.

#### OLS Diagnostics

Input Features:	CalEPA_RegressionTable	Dependent Variable:	DEGHOURDAY_FLOAT
Number of Observations:	887	Akaike's Information Criterion (AICc) [d]:	7782,134460
Multiple R-Squared [d]:	0,033050	Adjusted R-Squared [d]:	0,031957
Joint F-Statistic [e]:	30,248614	Prob(>F), (1,885) degrees of freedom:	0,000000*
Joint Wald Statistic [e]:	34,031955	Prob(>chi-squared), (1) degrees of freedom:	0,000000*
Koenker (BP) Statistic [f]:	77,523615	Prob(>chi-squared), (1) degrees of freedom:	0,000000*
Jarque-Bera Statistic [g]:	170,956474	Prob(>chi-squared), (2) degrees of freedom:	0,000000*

Figure 25: Ordinary Least Squares result for CalEPA UHII and Aggregated Urban Climatic Classes

Regression Equation:

$$(1) \quad \text{CalEPA UHII} = -2.756451(\text{Aggregated Urban Climatic Map}) + 19.403551$$

The second Ordinary Least Squares model uses the projected wind speed values from the National Renewable Energy Laboratory to test whether the wind variable is a significant key variable that is a missing component in the linear regression model. The resulting  $R^2$  value for the second model including the wind variable was 0.314852. While the resulting  $R^2$  value indicates that the aggregated urban climatic map with the wind variable is still not a best fit, the result indicates that the wind variable is possibly one of the key exploratory variables that is missing between the aggregated urban climatic map when comparing the model with the CalEPA UHII model. Figure 26 shows the results of the second Ordinary Least Squares model, which includes the projected wind speed classes. The regression equation to model the best fit line is also given below.

### OLS Diagnostics

Input Features:	CalEPA_RegressionTable	Dependent Variable:	DEGHOURDAY_FLOAT
Number of Observations:	887	Akaike's Information Criterion (AICc) [d]:	7478,570201
Multiple R-Squared [d]:	0,314852	Adjusted R-Squared [d]:	0,313302
Joint F-Statistic [e]:	203,116099	Prob(>F), (2,884) degrees of freedom:	0,000000*
Joint Wald Statistic [e]:	223,324823	Prob(>chi-squared), (2) degrees of freedom:	0,000000*
Koenker (BP) Statistic [f]:	171,083744	Prob(>chi-squared), (2) degrees of freedom:	0,000000*
Jarque-Bera Statistic [g]:	51,580129	Prob(>chi-squared), (2) degrees of freedom:	0,000000*

Figure 26: Ordinary Least Squares result for CalEPA UHII, Aggregated Urban Climatic Classes, and Projected Wind Speed Values

Regression Equation:

$$(2) \quad \text{CalEPA UHII} = -7,539121(\text{Aggregated Urban Climatic Class}) - 16,025709(\text{Wind Speed Classification}) + 33,739969$$

The residuals from the second Ordinary Least Squares model are also mapped as an output from the Ordinary Least Squares tool. The residuals visualize the difference between the actual data points and the projected data points that is plotted as a result of the linear regression equation. These results can be used to verify the accuracy of a model or dataset and any potential missing variables with a reference dataset. Figure 27 shows the residuals generated from the aggregated urban climatic map and projected wind dataset with the reference CalEPA UHII model.

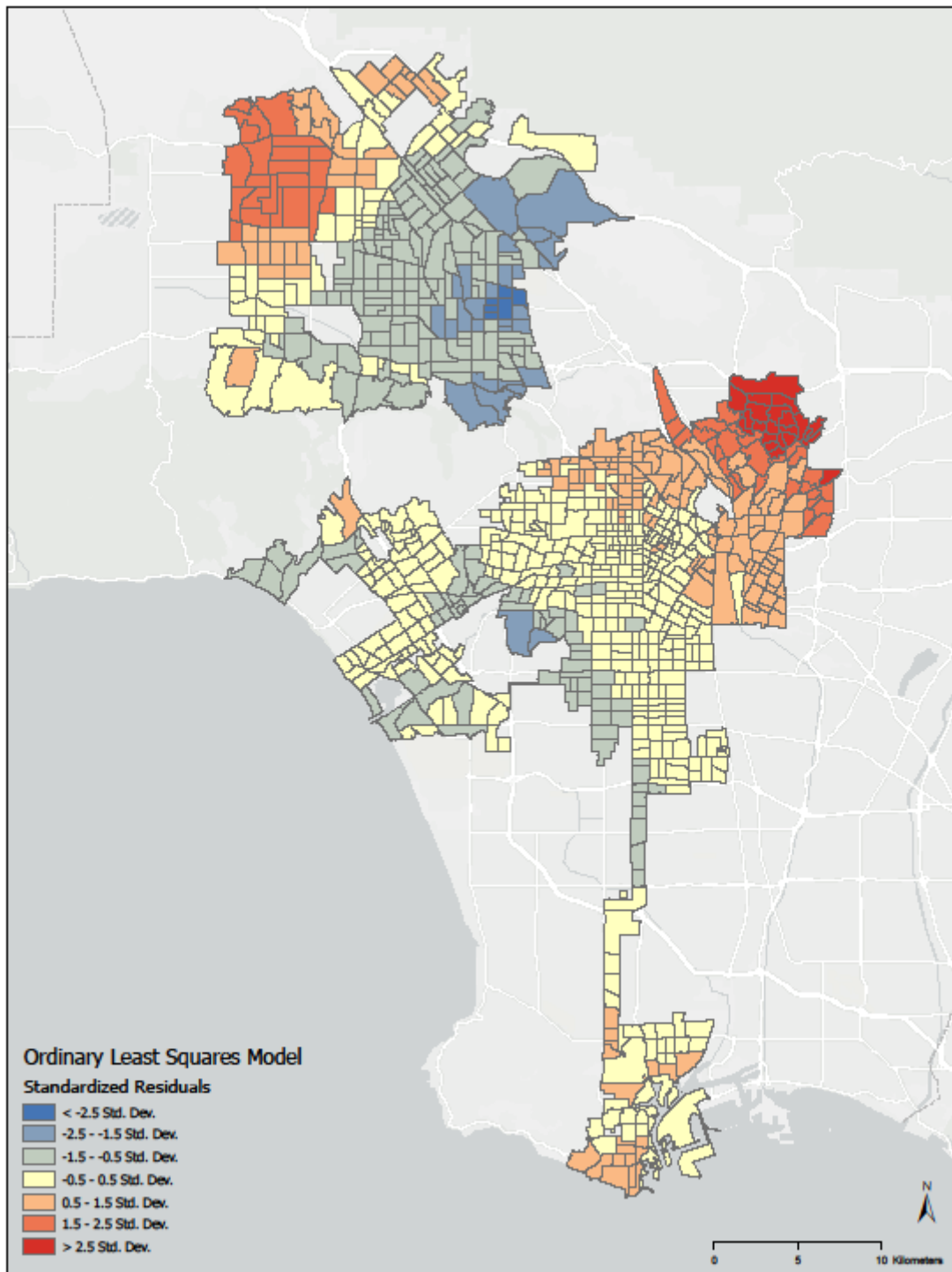


Figure 27: Ordinary Least Squares Standardized Residuals

#### **4.5. Urban Climatic Map with Wind Layer and Prevailing Wind Information**

The final urban climatic map takes into account the prevailing wind information from the National Centers for Environmental Information and the projected wind speed information from the National Renewable Energy Laboratory. The prevailing wind information is presented as wind arrows above the weather station that the wind observations were recorded. Figures 28 and 29 show the wind roses generated by the Python script for each of the weather stations in the Los Angeles city vicinity, separated by the summer months and the Santa Ana wind months. Figure 30 shows the locations of the NCEI weather stations where the wind speeds and directions were observed. Figures 31 and 32 show the wind roses created from the wind dataset observed at each of the weather stations shown in figure 30. The summer months are defined as the months of June to August and the Santa Ana wind months are defined from October to December. The projected wind speed information is reclassified into classes based on the wind velocity categories presented in the wind prospector web application. Figure 33 shows the final urban climatic map for Los Angeles including the summer month wind information, while figure 34 shows the final urban climatic map for Los Angeles with the Santa Ana month wind conditions.

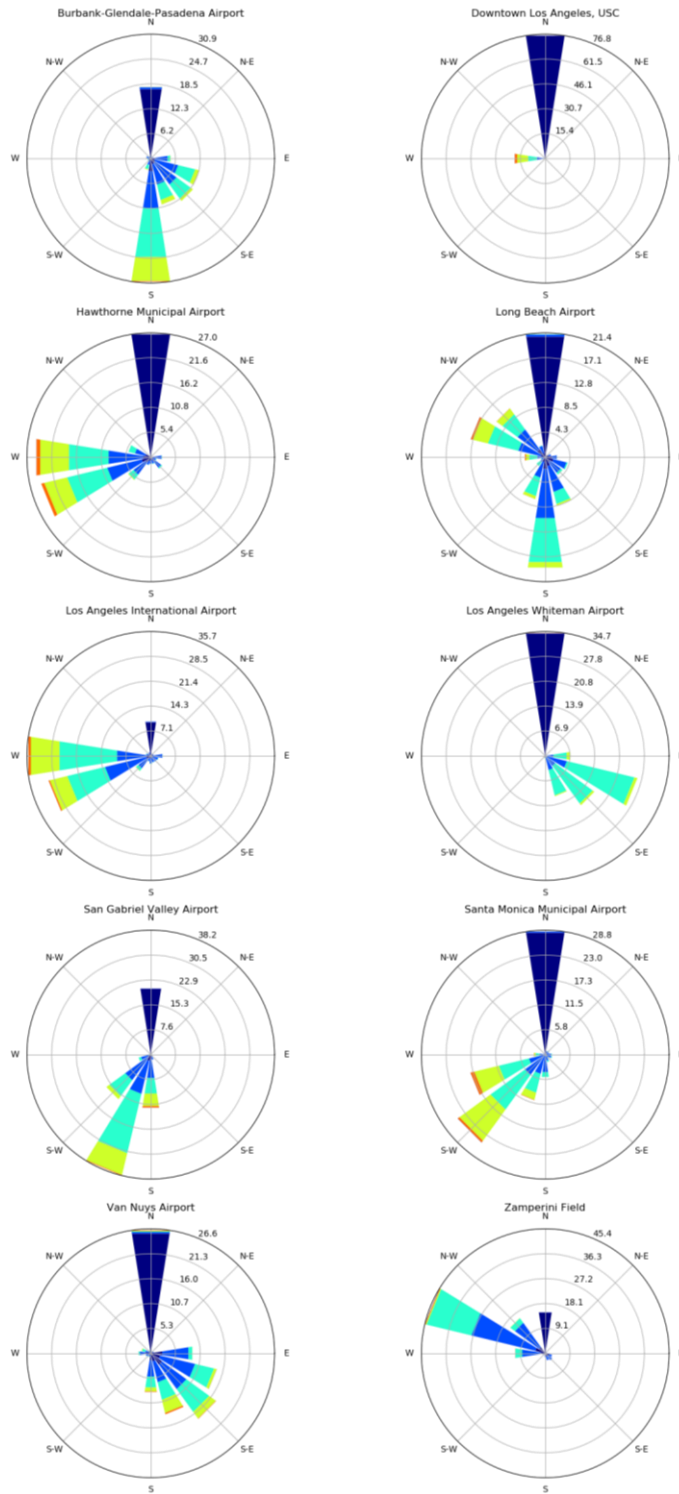


Figure 28: Summer Months Wind Roses



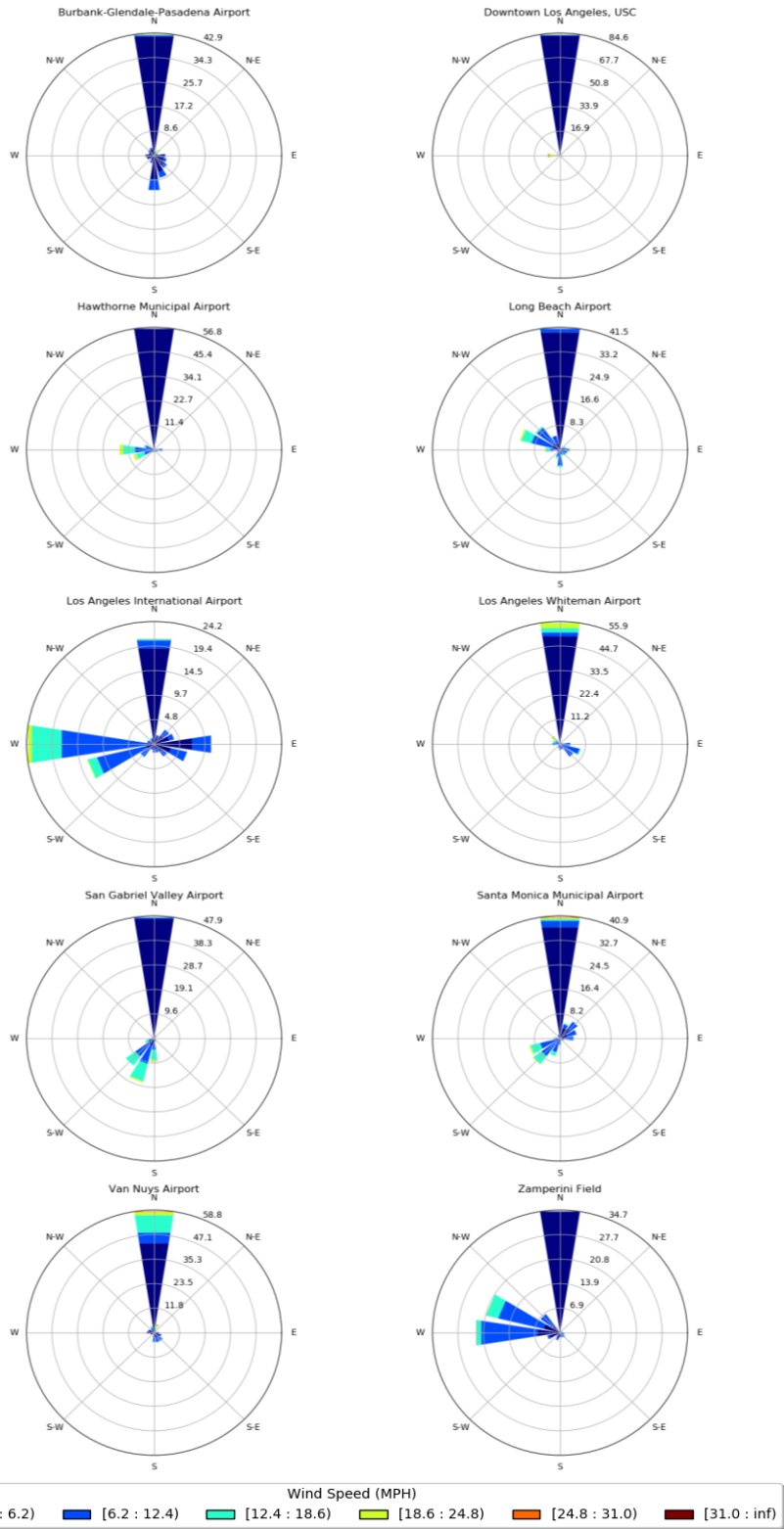


Figure 29: Santa Ana Wind Months Wind Roses

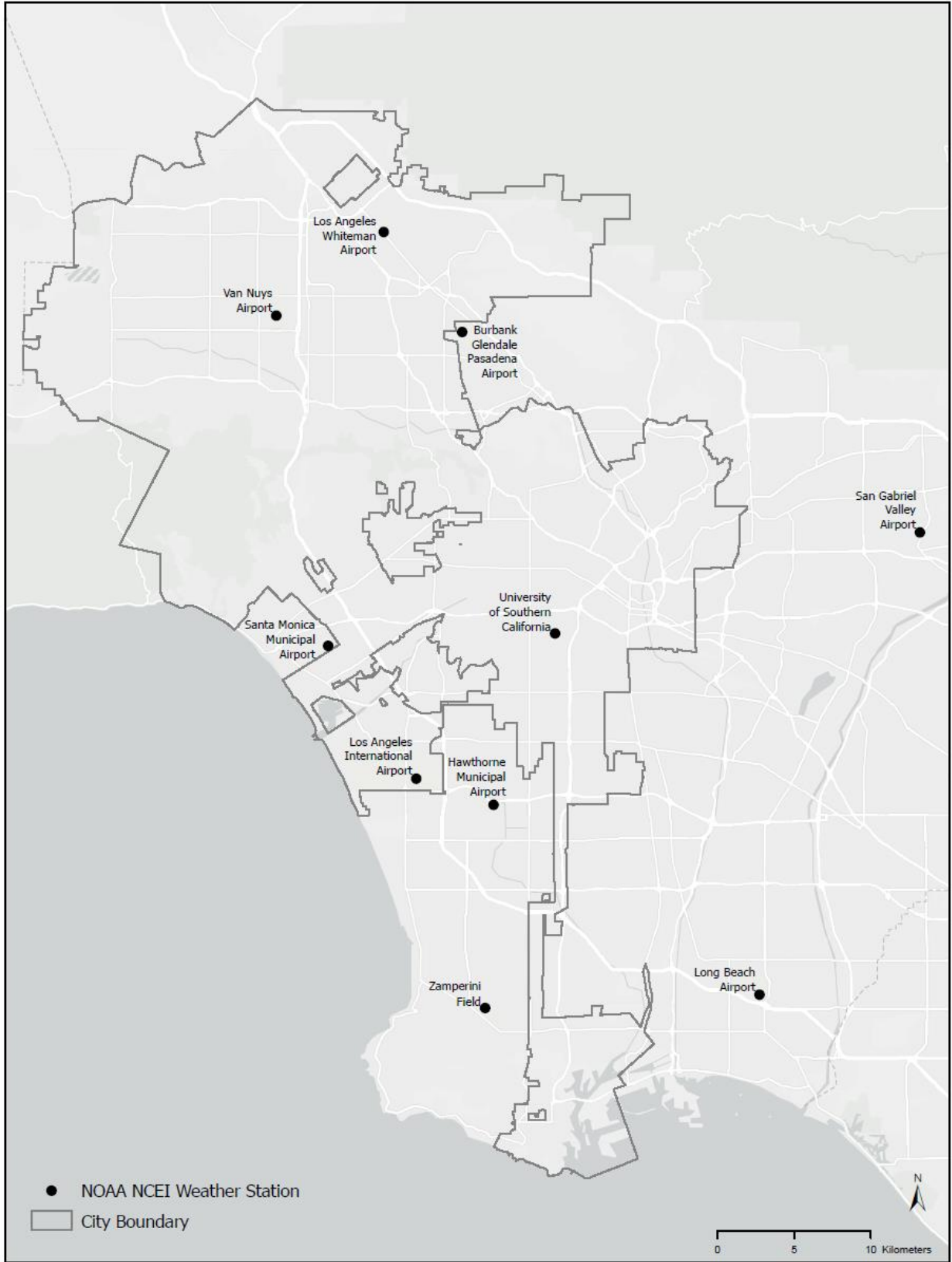


Figure 30: Weather Station Locations

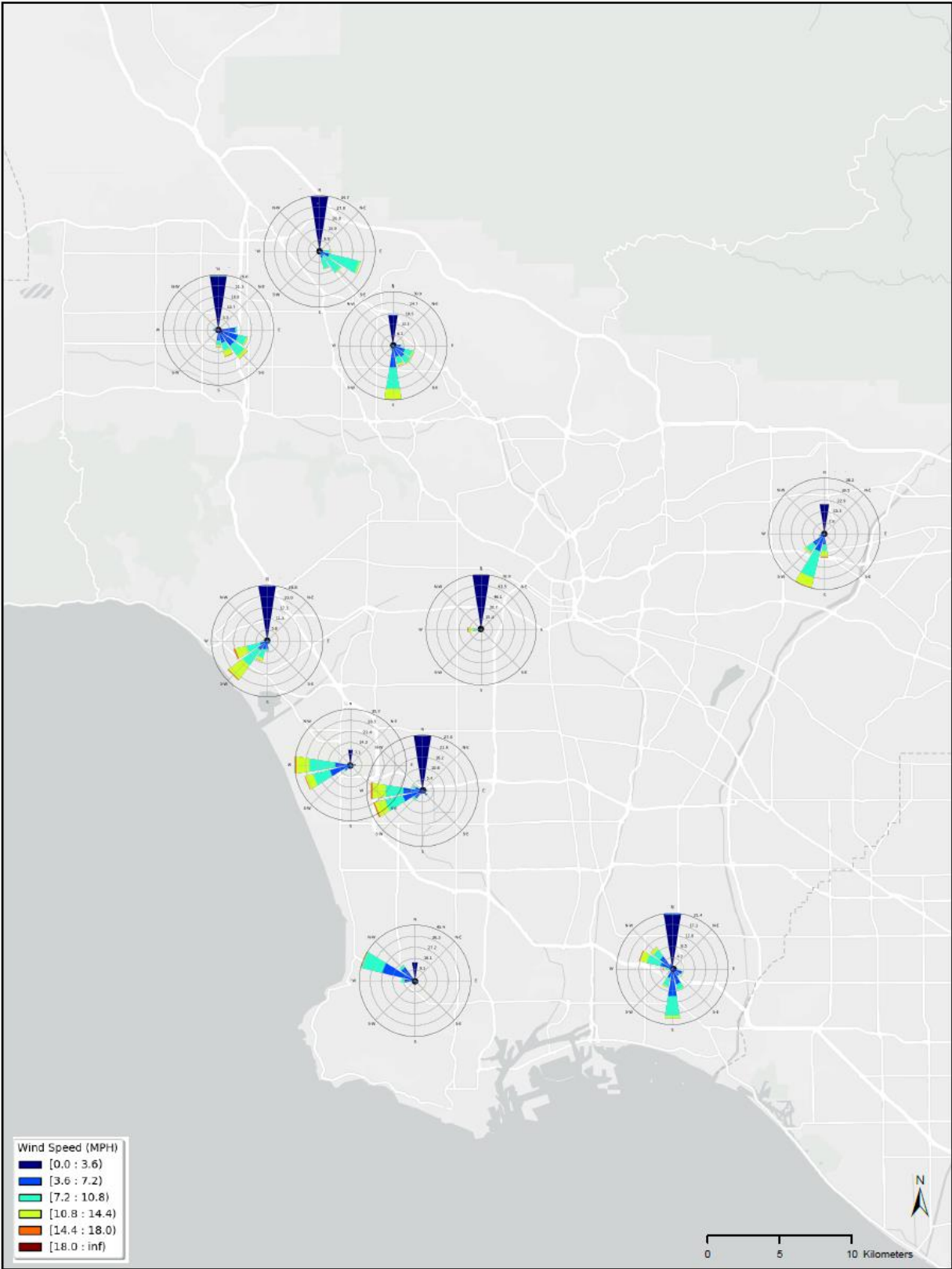


Figure 31: Summer Month Wind Roses

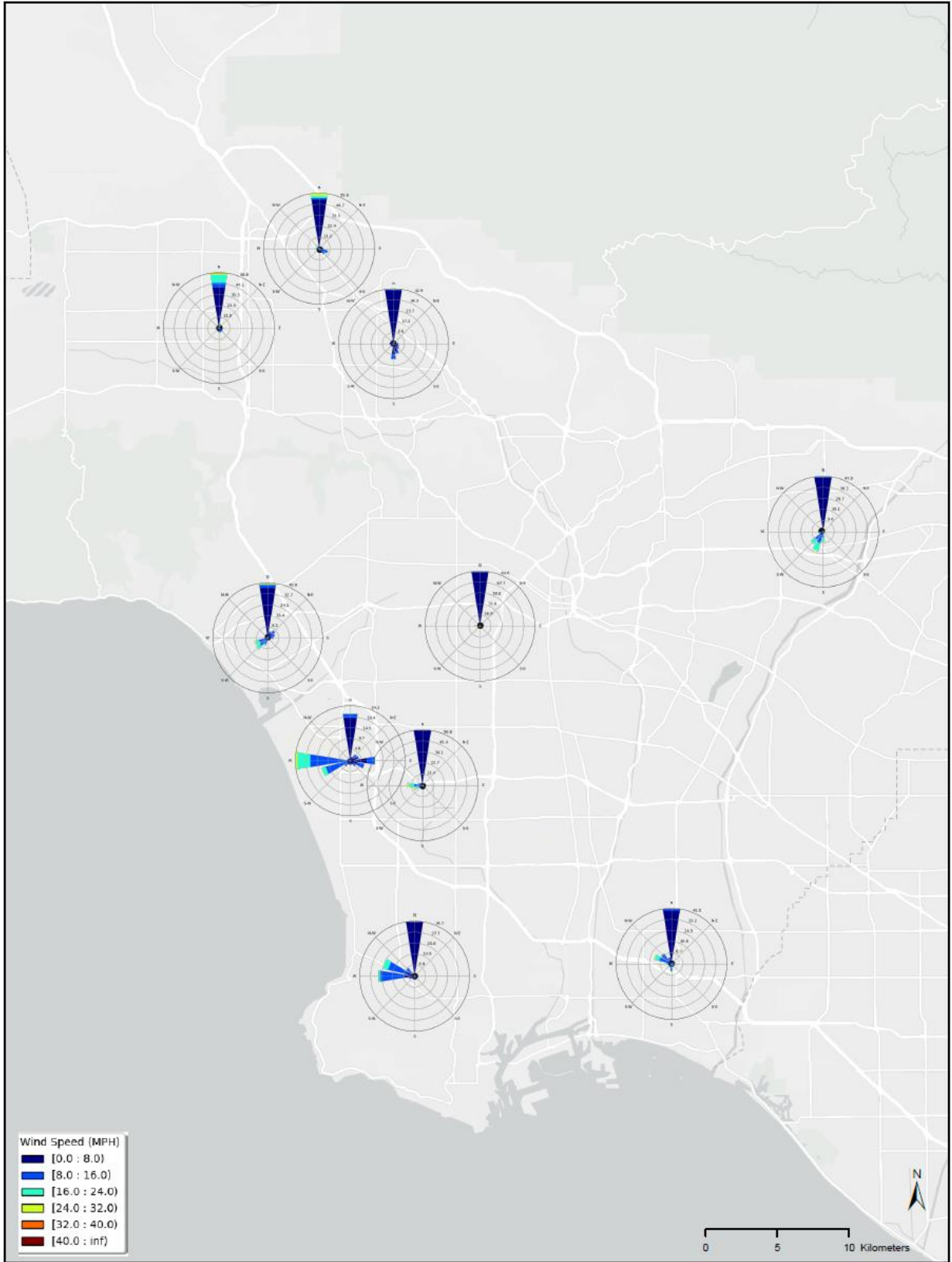


Figure 32: Santa Ana Months Wind Roses

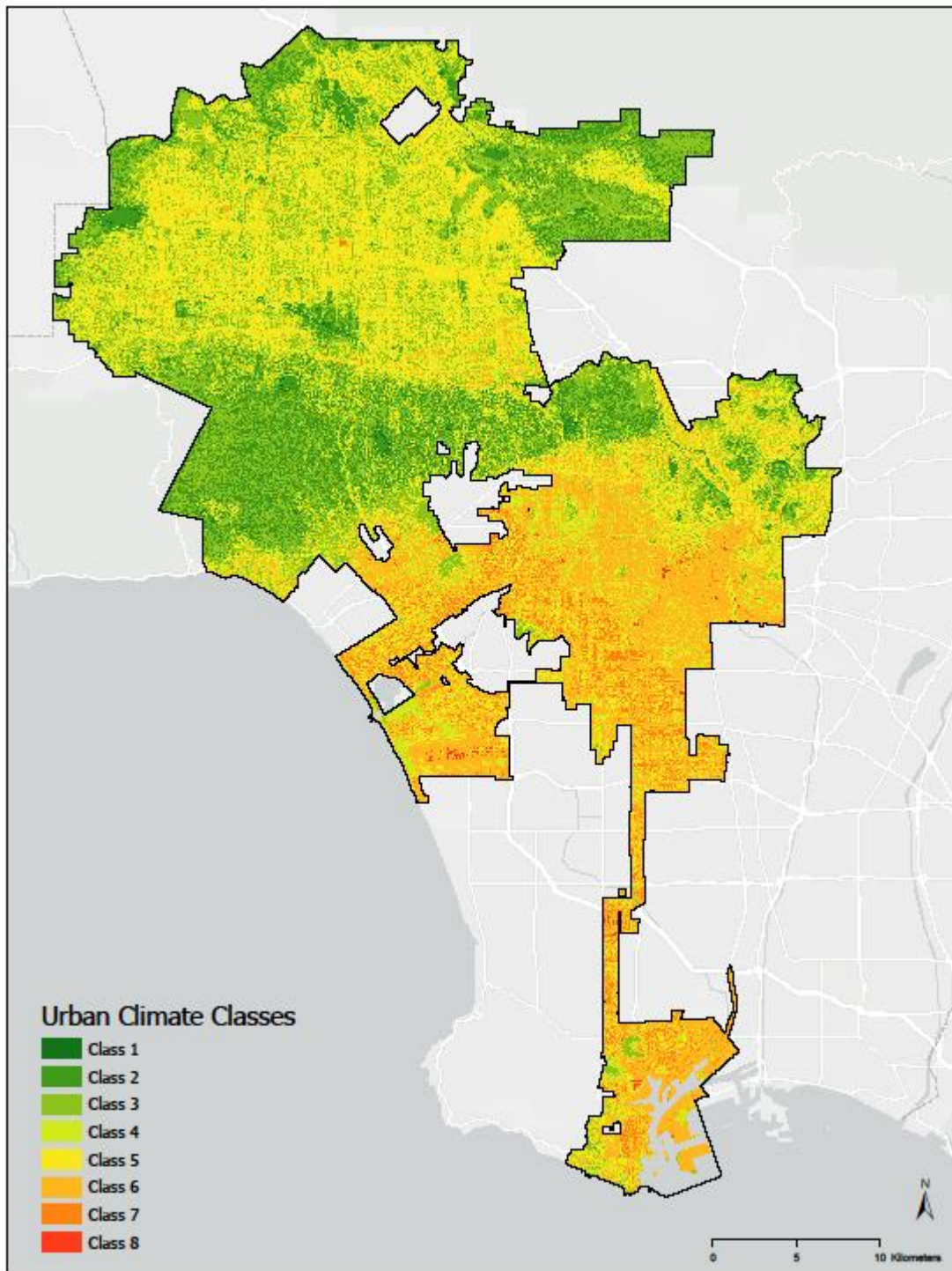


Figure 33: Final Urban Climatic Map without Wind Layer

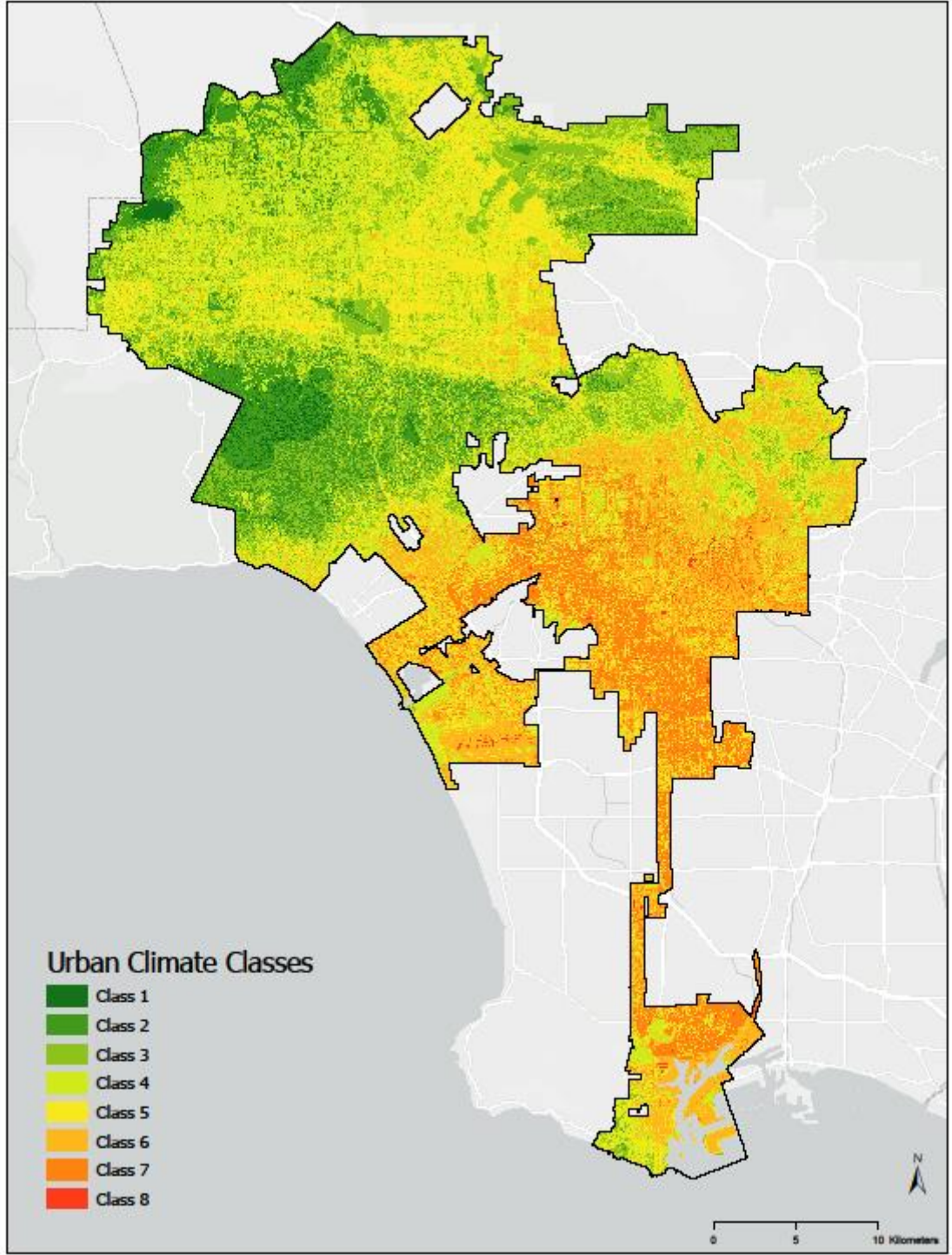


Figure 34: Final Urban Climatic Map with Wind Layer

## **Chapter 5 - Discussion and Conclusion**

The purpose of this project is to develop an urban climatic map for the city of Los Angeles and test its accuracy and effectiveness as an urban heat island visualization model by comparing it with another urban heat island model for the region. Referencing the classification scheme developed by Ng and Ren (2012) for the urban climatic map of Hong Kong, the urban climatic map was developed by classifying variables related to the thermal load and dynamic potential aspects, such as building volume, vegetative cover, ground cover, and distance from open areas. This chapter highlights observations made about the results of the urban climatic map, how the urban climatic map compares to the results of other urban heat island studies done in the Los Angeles area, addresses limitations, and proposes possible future work to improve the urban climatic map for Los Angeles and in other similar regions around Southern California.

### **5.1. Observations**

The majority of the lower urban climate classes are distributed in the hillside areas of Los Angeles, such as the Santa Monica Mountains, the San Gabriel Mountains, and the areas of Griffith Park. These results are expected as the low urban climatic classes describe open spaces and other areas with little to no urban development. Similarly, we see higher urban climatic classes in more heavily urbanized areas, such as Downtown Los Angeles. The taller buildings and low vegetative cover, combined with mostly impervious surfaces would increase the thermal load and reduce the dynamic potential of the area, which can be represented through the higher urban climatic classes.

The urban climatic classes also reveal that on average, various residential communities, such as San Pedro and South Los Angeles, are classified much higher than other more heavily urbanized places containing commercial and industrial development. Typically, these

neighborhoods experience higher temperatures and possible greater urban heat island effect due to the topography, where nearby ranges block the sea breeze from blowing into these communities. The Palos Verdes Ranges prevent westward sea breezes from blowing into San Pedro, while the Baldwin Hills restrict sea breezes from blowing into the South Los Angeles communities to the east. The final urban climatic map including the wind speed classification layer visualizes these effects with higher classification values.

The elevation appears to have the biggest weight when looking at the complete urban climatic map, with urban climatic class changes defined by the classification scheme used in the topography layer. be weighted heavily. When comparing residential areas of different elevations, higher urban climatic classes are found in low elevations, such as in South Los Angeles, and lower classes are found in the San Fernando Valley, at a higher elevation. Areas of Wilmington are also classified with higher urban climatic classes, possibly due to its sea level elevation.

The creation of wind roses was done to replicate the work done by Ng and Ren (2012) on their urban climatic map, where they used wind speed and direction observations to illustrate prevailing wind information, and wind models to show air ventilation paths for the region. Due to the unique wind conditions of Los Angeles, it is more appropriate to show the wind roses, rather than just wind arrows, in order to fully understand the prevailing wind conditions of the region. As a result, to make the wind roses more noticeable on a map, the methodology was changed to show the wind speed and direction information as its own individual map, rather than integrate prevailing wind arrows within the urban climatic map itself.

Analyzing the results of the urban climatic map with other urban heat island studies of Los Angeles reveals several differences. The main difference that can be observed between the Los Angeles urban climatic map and other Los Angeles urban heat island studies is the locations



of where the most intense urban heat island events are occurring. In older studies, more intense urban heat islands were found to be focused around industrial and commercial areas, as shown in the works of Roth *et al.* (1989) and Dousset (1992). The materials used in industrial buildings and impervious surfaces kept temperatures warmer than residential areas within the same region. The results of the urban climatic map agree with a portion of these findings, where heavy commercial and industrial areas of Downtown Los Angeles and the communities of Wilmington and Harbor Gateway have a much higher urban climatic class than surrounding neighborhoods. However, it is not possible to compare the results of other neighborhoods identified in the Roth *et al.* and Dousset studies, as they are separate cities and neighborhoods outside the Los Angeles city boundaries and are not included in the Los Angeles urban climatic map.

More recent studies, such as the one completed by Hulley *et al.* (2019) analyzes neighborhood and city vulnerabilities to the urban heat island effect and analyzed the land surface temperatures during the day and night. Using the National Aeronautics and Space Administration's (NASA) new Ecosystem Spaceborne Thermal Radiometer Experiment on Space Station (ECOSTRESS), the researchers reveal that areas containing a large amount of materials with high heat capacity, such as concrete, asphalt and waterbodies were able to absorb large amounts of heat during the day and reradiate it during the night, which increases the overall temperatures and the urban heat islands within these areas (Hulley *et al.*, 2019). These areas include the various airports scattered around the city, the port area, and valley areas, such as areas in the San Fernando and San Gabriel Valley.

While the results of the urban climatic map and Hulley *et al.* (2019) both find that the port areas and the industrial areas of Downtown Los Angeles experience much more intense urban heat islands, proved by the higher temperatures detected by ECOSTRESS in Hulley *et al.*

(2019) and the higher urban climatic classes for these areas from the Los Angeles urban climatic map. However, the urban climatic map fails to classify most of the San Fernando Valley with higher urban climatic classes, when compared to the high temperatures detected in the San Fernando Valley by the ECOSTRESS program. The urban climatic map also classifies much of the residential neighborhoods of South Los Angeles with very high urban climatic classes, where there are not any high the ECOSTRESS program does not. These two issues can be explained by the elevation possibly having a much higher weight when creating the urban climatic map for Los Angeles and is discussed further in the limitations section.

## **5.2. Limitations**

While the groundwork for the Hong Kong urban climatic map presented by Ng and Ren in their 2012 study can be easily replicated, the methodology can only be used to guide the basis of developing urban climatic maps for other cities, such as Los Angeles. The complexities of the urban climatic map, the different input datasets, and different variable classifications and weightings would lead to inaccurate urban climatic modeling when the same model is applied to different cities around the world. For example, the urban climates used to describe the compact, dense building forms in a humid city such as Hong Kong would not accurately translate to describing the urban climates of a semi-arid, urban sprawl city such as Los Angeles. Variables such as wind are also difficult to model and include in the urban climatic map, due to its complexity and how wind interacts and move through the environment. It is important to understand the issues and inaccuracies that may arise when creating the urban climatic map for Los Angeles.

The major limitation of the Los Angeles urban climatic map is the weighting and classification used to classify each layer. As this project uses the classification scheme from the

Hong Kong urban climatic map done by Ng and Ren (2012), it cannot accurately represent the urban climate of the Los Angeles region. Hong Kong is characterized by tall, highly dense building forms, while Los Angeles is characterized by having a more uniform, medium to low density urban environment. For example, the classification used is tailored to accurately model the high rise, dense building forms of Hong Kong, but it may not accurately represent the uniform low to medium building densities of Los Angeles. These differences would mean that due to the values used for classification, some layers are weighted more heavily than others.

The weighting limitation can be observed by looking at the current system used to classify and weight each of the layers in the urban climatic map. Some variables, such as the building volume variables, are classified with values ranging from 0 to 5, while the vegetation variable for the thermal load aspect is only classified using a value of -1 and 0. The classification range used in the building volume layer is much higher than the other layers, which potentially leads to a greater impact on the final urban climatic class value when all the layers are added together using raster calculator. The values found in the building volume layer can shift a specific pixel's final urban climatic class number, where on the other hand, the vegetation layer classification value of -1 would generally not change or alter any of the pixel's urban climatic class number. This limitation is an issue that must be addressed in future urban climatic map methodologies, where layers have different weights on the overall urban climatic map based on how many individual values were assigned as part of the classification process.

The classification of the building volume layer used for the Hong Kong urban climatic map is not suitable to describe the building volumes found in Los Angeles. Ng and Ren (2012) utilized sky view factors to assign classification values for the building volume layer. Sky View Factor describes how much the visible sky can be viewed at a measured point, provided as a

ratio. This method is one of the more common methods of studying urban morphology and is often used to describe a three-dimensional built environment feature as a two-dimensional variable to be used in urban models (Middel *et al.* 2018). The sky view factor can also be correlated with urban heat island intensity, as shown in Oke (1982). This analysis would be necessary to correctly assign classification values to the building volume percentages, so that the classifications can accurately describe the built environments of Los Angeles and be weighted correctly in relation to the other layers in the urban climatic map.

Calculating the vegetation layers for both the thermal load and dynamic potential layers utilized NDVI to determine the presence of vegetation in the area. However, the NDVI is a relatively simple index which is a representation of the “greenness” of an object. This means that any object that can reflect the same red, green, and near-infrared wavelengths as the amount reflected from vegetation would result in the same NDVI values calculated. A study by Huete and Jackson (1988) found that soil influences can be as significant as atmospheric effects on remotely sensed indices and would need to be corrected in order to calculate accurate vegetation values. Improving the vegetation layer for the Los Angeles urban climatic map can involve using other vegetation indices, such as the Soil-Adjusted Vegetation Index (SAVI) and the Modified Soil-Adjusted Vegetation Index (MSAVI) developed by Qi *et al.* (1994), in order to reduce the influence of soils in vegetative cover calculations.

Topography appears to have the most influence on the Los Angeles urban climatic map. The classification used by Ng and Ren (2012) are calibrated for Hong Kong, as most of the built environment is at sea level, along the coasts. Hong Kong’s urban development is concentrated around the coastal regions and the lower elevations, where the terrain is flat to build upon. The classification used by Ng and Ren (2012) reflects this. Los Angeles, on the other hand, has urban

development several hundred meters above sea level. This would result in areas, such as the San Fernando Valley, having negative classification values assigned using the Hong Kong urban climatic map classification scheme, and underestimate the thermal load of the region. This can be observed when comparing the results of the Los Angeles urban climatic map and how the low urban climatic classes do not match the results from the Hulley *et al.* (2019) study. The results of the ECOSTRESS land surface temperature experiment shows higher temperatures in the San Fernando Valley, compared to the rest of the city. However, from the Los Angeles urban climatic map, due to the classification of the elevation, the urban climatic classes suggest that the lower elevations of South Los Angeles cause the urban climatic classes to be higher, while areas where we expect much higher susceptibility to the urban heat island are assigned lower classification values due to the valley's elevation of a few hundred meters above sea level.

The elevation range in Hong Kong is also much smaller compared to the elevation range found in the city of Los Angeles. The lowest point in Hong Kong is at sea level, along the coastlines, while the highest point is Tai Mo Shan, rising 957 meters above sea level. On the other hand, the lowest point in Los Angeles is the Wilmington neighborhood, found several meters below sea level, while the peak of Mount Lukens is the highest point in the city, rising more than 1540 meters above sea level. More research must be done to develop a more appropriate classification scheme and have possible weights assigned to the layer to accurately describe the elevation ranges of Los Angeles and its impact on the thermal load.

Wind conditions are not accurately represented in the Los Angeles urban climatic map. In the Hong Kong urban climatic map, Ng and Ren (2012) performed various wind model tests, to model possible air ventilation paths to understand how wind could move through the region. These variables are considered to explain where the urban heat island effect can intensify and

where this effect may be negated as a result of the wind. The wind data used for the Los Angeles urban climatic map is a projected wind speed map, which shows the potential wind speeds, and therefore, not an accurate model of the wind speeds that have been observed during the time period.

The geography of Hong Kong allows sea breezes to affect the majority of the urban development found within the region. These effects can be represented by both the wind conditions and the proximity to coastlines layer. Los Angeles, on the other hand, only contains very few coastal communities which benefits from the sea breeze, such as the Westside communities of Venice and Santa Monica. San Pedro, on the other hand, does not receive as much of a benefit from the sea breeze, as the Palos Verdes Hills block onshore flow to cool the region. For the Los Angeles urban climatic map, the proximity to coastlines would need to be adjusted or combined with the wind data to develop more accurate weights for classification.

The wind roses generated from the Python script show the wind speeds and the frequencies in which they occur. This was done to identify the prevailing wind speed and direction of the region. However, the wind roses do not distinguish between wind patterns during the day and night. This is an issue, as the Los Angeles area typically experiences onshore flow during the day, and offshore flow during the night. In the wind roses, the reversing wind patterns can sometimes appear to have the same frequencies in multiple directions, meaning it can be difficult to identify the prevailing wind directions just from one wind rose at each location. This issue can be solved by separating daytime wind observations and nighttime observations and creating separate wind roses for each condition.

The effects of Santa Ana wind conditions are not modeled by the Los Angeles urban climatic map using the methodology for the Hong Kong urban climatic map. As a result, the Los

Angeles urban climatic map may not represent the effects on the urban heat island during these months. Temperatures often rise during the Santa Ana wind months while the wind strength can have the potential to increase the dynamic potential of the region. More research will need to be done to identify the effects and see which effects are the strongest during the Santa Ana months.

Due to the coverage and extent of the datasets used, the Los Angeles urban climatic map covers only areas within the Los Angeles city boundaries. The unique shape of the city results in the exclusion of many neighborhoods along the coast and inland communities where there is more industrial urban development. Cities that border Los Angeles may contain elements that can affect the overall thermal load and dynamic potential, and possibly urban heat island effects along the boundaries of Los Angeles. Many other urban heat island studies have analyzed Los Angeles as a region, including analyzing neighborhoods surrounding the city boundaries. As shown in the observations, it was not possible to validate the results of the urban climatic map with the studies done by Roth *et al.* (1989) and Dousset (1992), as they identified neighborhoods outside the city of Los Angeles. This issue can be resolved in future studies by analyzing a larger area, such as including the surrounding neighborhoods, or even the entire Los Angeles county to calculate the urban climatic classes for the city.

The linear regression model completed for this project compares how well the Los Angeles urban climatic map and potential missing variables fit with the CalEPA's Urban Heat Island Index, the established study used as the reference for validation. The Los Angeles urban climatic model along with the NREL's projected wind speed data resulted in a  $R^2$  value of approximately 0.31, which indicates that the two variables can account for 31% of the variability between the CalEPA model and the urban climatic map. However, the low  $R^2$  value indicates there are many missing variables that have not been accounted for. These variables can include

meteorological or population variables used in the CalEPA UHII model. While the urban climatic map is not a temperature-based classification, temperature can also be a key missing variable that can account for the missing 69% variability between the two models.

### **5.3. Future Work**

Future work on the Los Angeles urban climatic map involves addressing the limitations of the map and the inclusion of other variables used in the CalEPA UHII model, along with other urban climatic maps developed in the past. Further work would focus on differentiating between urban and rural areas, accounting for missing variables, and accurately assigning weights and classifications of variables used in the urban climatic map for Los Angeles. This can be accomplished through analyzing Köppen climate classifications between the cities and utilizing meteorological and climate models to analyze short-term weather conditions and long-term climate. Comparison by individual variables in the regression model would also find which individual variables have a much higher influence and greater weight in the city for the urban climatic map. The wind layer used in the Los Angeles urban climatic map makes it difficult to accurately model the wind conditions and its effect on the urban climates within the region. Future work would also propose methods and other workflows to accurately model the complex wind conditions in Los Angeles. Finally, the urban climatic map must be comprehensible to stakeholders such as urban planners, who will ultimately develop policies, best use practices, or recommendations to mitigate the effects of the urban heat island.

It is important to differentiate urban and rural areas within the city when discussing the urban climate and the urban heat island. The urban heat island is often defined as the temperature increase and warming observed in an urbanized setting. As a result, the urban climatic map for Los Angeles treats the region as one homogenous built environment. Future work on the urban



climatic map would segment these areas further, where areas of Los Angeles can be classified as urban or rural. One approach to differentiating between urban and rural areas is using Local Climate Zone classification. According to Stewart and Oke (2006), these local climate zones are classified based on regions of uniform surface cover, structure, material, and human activity. By weighting the urban climate classes based on the local climate zones proposed by Stewart and Oke, the urban climatic map can differentiate between urban and rural areas and apply the urban climatic classes accordingly.

The weighting of each layer as a result of the classification process must be addressed, which results in some layers of the urban climatic map that have a disproportionately higher weight than other layers. Under normal circumstances, the seven variables used in the final urban climatic map with the wind layer, each variable would be weighted equally at approximately 14.3%. In future work on the Los Angeles urban climatic map, the weighting can be adjusted for each layer based on classification range used in each layer. As an example, the building volume layer can be reweighted to match the classification values used in other layers in the urban climatic map. Instead of assigning integer classification values from 0 to 5, the reweighted values would then be assigned decimal values between 0 to 1, to match the classification values of -1 and 0 used in the vegetation layer. Since the final urban climatic map is a reclassified raster based on the results of a raster calculator process, it would not be an issue to use decimals or non-integer values in the classification. The urban climatic classes used in the map are the result of a reclassification of a range of values resulting from the raster calculator process into eight different classes.

The weighting and classification of the urban climatic map layers can also be customized by climate classification. When looking at potential future studies where much larger regions

cover multiple Köppen climate classifications, it is important to understand the potential effects that each climate classification can have on the urban heat island effect. Under the Köppen climate classification scheme, Hong Kong's climate is described as humid subtropical, while Los Angeles has a Mediterranean climate, typically characterized by dry conditions. The two climates are significant enough that the weights and classifications must be adjusted to account for these differences, in order to accurately represent the regional climate's impact to the urban heat island. These climatic differences are not limited to the regional scale, but to the local scale as well. Microclimates also exist within the Los Angeles area, with some of the coastal communities experiencing much cooler temperatures than areas up in the San Fernando valley, where the warmest temperatures in the entire city are often observed. In addition to customizing weights by climate classification, future work on the urban climatic map for Los Angeles would also focus on the microclimatic variations observed in the city.

Missing variables must be accounted for to fully develop an accurate model describing the urban climate of the region. One example is the additional variables used in the CalEPA UHII model that are not present in the Los Angeles urban climatic map, including population density and other meteorological and climatological variables such as temperature, solar radiation, and surface albedo. Urban climatic maps such as the one developed for Berlin, Germany, and Arnhem, Netherlands utilize air temperatures during different times of the day as an input variable for their analysis. Regional variables specific to a region should also be considered to model certain characteristics. For Los Angeles, this could include analyzing air pollution and its impact to the urban heat island effect and other urban developments.

In addition to identifying and including missing variables between the urban climatic map and the CalEPA UHII model, work must also be done to compare each of the individual

variables used in both models. Using the ordinary least squares model, we can identify the missing exploratory variables in more detail, and identify which variables are more significant to Los Angeles, compared to the variables used in the Hong Kong urban climatic map. A one to one comparison of the variables would be able to reveal variables which have more significance to the Los Angeles region and identify variables which do not have a significant impact in the region. This information would ultimately help with the reweighting and reclassification of the layers for future urban climatic maps of Los Angeles.

One of the biggest limitations of the Los Angeles urban climatic map is the wind variable. The complexity of wind makes it difficult to accurately model wind patterns, especially for Los Angeles, which experiences daily onshore and offshore flow, and the seasonal Santa Ana winds. Future work could improve on the wind data used for the current Los Angeles urban climatic map by using higher spatial and temporal resolution data. Wind data interpolation from weather station observations is another option that can be taken. This can also help distinguish between day and nighttime wind conditions and between summer months and Santa Ana month wind conditions.

The wind variable in the urban climatic map would also need to describe friction surfaces, such as commercial buildings or terrain. And how moving air flows through the city, interacting with these built environments. These friction surfaces can alter air flow, by changing the wind speed or direction, which can impact how heat can be transported throughout the city and impact the urban heat island. These changing wind observations can be visualized through three-dimensional modeling of wind profiles and built environments which can help analyze the horizontal and vertical wind vectors as they pass through buildings and other terrain. Improvements in technology in the future can potentially allow for accurate, real-time wind

modeling, which can model the changes friction surfaces can have on the wind. This can lead to quicker analysis and response on changing wind conditions within the microclimates.

Future work on the urban climatic map can utilize the improved technologies in the future, which leads to improved data richness which can be drawn upon to improve future urban climatic maps. This can include a higher frequency in which the data is collected, increased resolution of the data, or better, more efficient ways of ground truthing and validating the data. With the datasets available at the time of creating the initial urban climatic map for Los Angeles, the classes are describing based on the capture date of the 2017 LARIAC orthoimagery and is a snapshot of a point in time. Increased frequency of the observations and imagery capture can allow for the urban climatic classes to be modelled in real time and allow for immediate responses to issues, such as the increase in urban heat island within a specific microclimate in the city in an hourly or daily basis.

Urban climatic maps are intended to be used by urban planners to aid in their decision and policymaking to mitigate the effects of the urban heat island in their city. The urban climatic map draw from variables and datasets that are familiar to urban planners and other policy makers, such as land use, land cover, and building footprint information. It is important for urban planners to understand the urban climate of the region and its classifications in the map that they can easily understand, so the recommend policies and best use practices are applicable and suitable for the region.

Urban planners have different goals and priorities when planning for their cities, and while the urban climatic map proposes a somewhat standardized method for urban heat island studies, the implementation of policy and how the urban climatic classes are analyzed will differ by region. In many urban climatic map studies, such as the urban climatic map for Hong Kong,

an additional recommendations map is created based on the results of the urban climatic map. The urban climatic planning recommendations map for Hong Kong recategorizes the urban climate classes into five planning zones, with each zone contains a recommendation of action relating to urban heat island mitigation strategies. Similar methodologies can be adapted for other cities, such as Los Angeles, where planners can use the urban climate map to develop policies and prioritize specific areas of Los Angeles to mitigate the most intense urban heat island effects in the city.

#### **5.4. Conclusion**

The Los Angeles urban climatic map proposes a new methodology for urban heat island studies, as a standardized way to model urban heat island in a region, by replicating the methodology of other developed urban climatic maps. While there are many limitations as discussed for the Los Angeles urban climatic map, the groundwork established by urban climate researchers have been successful in other regions around the world, such as in Europe and Asia. The quantification of urban classes can aid urban planners understand their cities' urban morphology, which can lead to better urban policies and recommendations, such as those which can mitigate the effects of the urban heat island. While the methodology for the urban climatic map will need to be customized based on the region being analyzed, these adjustments to the variable classification and inclusion of other variables such as wind could improve the urban climatic map for future areas in the region, with the purpose of replicating a similar methodology for other cities in California. There are many environmental challenges that must be solved, and the hope is that the methodology proposed in this project can form the groundwork for solutions to mitigate such issues, such as climate change.

## References

- Arnfield, A. J. 2003. "Two decades of urban climate research: a review of turbulence, exchanges of energy and water, and the urban heat island." *International Journal of Climatology*, 23(1); 1–26.
- Baumuller, J., U. Hoffmann, U. Reuter. 1992. Climate booklet for urban development, Ministry of Economy Baden-Wuerttemberg (Wirtschaftsministerium), Environmental Protection Department (Amt fur Umweltschutz).
- California Environmental Protection Agency. 2015. Creating and Mapping an Urban Heat Island Index for California. CalEPA / Altostratus Inc. Agreement No. 13-001.  
<https://calepa.ca.gov/wp-content/uploads/sites/6/2016/10/UrbanHeat-Report-Report.pdf>
- Dousset, Bénédicte Marie. 1992. "Remote Sensing of Urban Microclimates and their Relationship to Land Use: A Case Study of the Los Angeles Basin." PhD diss., University of California, Los Angeles.
- Evans, J. M., & S. D. Schiller. 1996. "Application of microclimate studies in town planning: A new capital city, an existing urban district and urban river front development." *Atmospheric Environment*, 30(3), 361–364.
- Glickman, Todd S. 2000. *Glossary of Meteorology (2nd ed.)*. Boston: American Meteorological Society.
- Golany, G.S. 1996. "Urban design morphology and thermal performance." *Atmospheric Environment*, 30(3), 455-465.
- Harlan, S. L., A. J. Brazel, L. Prashad, W. L. Stefanov, & L. Larsen. 2006. "Neighborhood microclimates and vulnerability to heat stress." *Social Science & Medicine*, 63(11), 2847–2863.
- Huete, A. R., & Jackson, R. D. 1988. "Soil and atmosphere influences on the spectra of partial canopies." *Remote Sensing of Environment*, 25(1), 89–105.
- Holmer, B., U. Postgård, & M. Eriksson. 2001. "Sky view factors in forest canopies calculated with IDRISI." *Theoretical and Applied Climatology*, 68(1-2), 33–40.
- Imhoff, M. L., P. Zhang, R. E. Wolfe, & L. Bounoua. 2010. "Remote sensing of the urban heat island effect across biomes in the continental USA." *Remote Sensing of Environment*, 114(3), 504–513.
- Kim, H. H. 1992. "Urban heat island." *International Journal of Remote Sensing*, 13(12), 2319–2336.

- Kovats R. S. & H. Shakoor. 2008. "Heat Stress and Public Health: A Critical Review." *Annual Review of Public Health*, 29(1), 41-55.
- Landsberg, H. E. 1981. *The Urban Climate*. New York: Academic Press.
- Lemonsu, A., V. Vigié, M. Daniel, & V. Masson. 2015. "Vulnerability to heat waves: Impact of urban expansion scenarios on urban heat island and heat stress in Paris (France)." *Urban Climate*, 14(4), 586-605.
- Manley, G. 1958. "On the frequency of snowfall in metropolitan England." *Quarterly Journal of the Royal Meteorological Society*, 84(359), 70-72.
- Middel, A., J. Lukaszczuk, R. Maciejewski, M. Demuzere, & M. Roth. 2018. "Sky View Factor footprints for urban climate modeling." *Urban Climate*, 25(1), 120-134.
- Ng, Edward, and R. Chao, eds. 2015. *The Urban Climatic Map: A Methodology for Sustainable Urban Planning*. Milton Park, Abingdon, Oxon OX14 4RN: Routledge.
- Oke, T. R. 1982. "The energetic basis of the urban heat island." *Quarterly Journal of the Royal Meteorological Society*, 108(455), 1-24.
- Oke, T. R. 1988. "The urban energy balance." *Progress in Physical Geography*, 12(4), 471-508.
- Oke, T. R. 1995. "The Heat Island of the Urban Boundary Layer: Characteristics, Causes and Effects." *Wind Climate in Cities*, 81-107.
- Office of Los Angeles Mayor. March 2018. Resilient Los Angeles. <https://www.lamayor.org/sites/g/files/wph446/f/page/file/Resilient%20Los%20Angeles.pdf>.
- Parker, D. E. 2009. "Urban heat island effects on estimates of observed climate change." *Wiley Interdisciplinary Reviews: Climate Change*, 1(1), 123-133.
- Peel, M. C., B. L. Finlayson, B. L., & T. A. McMahon. 2007. "Updated world map of the Köppen-Geiger climate classification." *Hydrology and Earth System Sciences*, 11, 1633-1644.
- Qi, J., A. Chehbouni, A. R. Huete, Y. H. Kerr, and S. Sorooshian. 1994. "A Modified Soil Adjusted Vegetation Index." *Remote Sensing of Environment*, 48, 119-126.
- Reid, C. E., M. S. O'Neill, C. J. Gronlund, S. J. Brines, D. G. Brown, A. V. Diez-Roux, & J. Schwartz. 2009. "Mapping Community Determinants of Heat Vulnerability." *Environmental Health Perspectives*, 117(11), 1730-1736.
- Ren, C., K. L. Lau, K. P. Yiu, & E. Ng. 2013. "The application of urban climatic mapping to the urban planning of high-density cities: The case of Kaohsiung, Taiwan." *Cities*, 31, 1-16.

- Rosenfeld, A. H., H. Akbari, J. J. Romm, & M. Pomerantz. 1998. "Cool communities: strategies for heat island mitigation and smog reduction." *Energy and Buildings*, 28(1), 51–62.
- Roth, M., T. R. Oke, & W. J. Emery. 1989. "Satellite-derived urban heat islands from three coastal cities and the utilization of such data in urban climatology." *International Journal of Remote Sensing*, 10(11), 1699–1720.
- Santamouris, M. 2019. "Mitigating the Local Climatic Change and Fighting Urban Vulnerability." *Minimizing Energy Consumption, Energy Poverty and Global and Local Climate Change in the Built Environment: Innovating to Zero*, 223–307.
- Sarrat, C., A. Lemonsu, V. Masson, & D. Guedalia. 2006. "Impact of urban heat island on regional atmospheric pollution." *Atmospheric Environment*, 40(10), 1743–1758.
- Solecki, W. D., C. Rosenzweig, L. Parshall, G. Pope, M. Clark, J. Cox, & M. Wiencke. 2005. "Mitigation of the heat island effect in urban New Jersey." *Environmental Hazards*, 6(1), 39–49.
- Stewart, I. D., & T. R. Oke. 2012. "Local Climate Zones for Urban Temperature Studies." *Bulletin of the American Meteorological Society*, 93(12), 1879–1900.
- Stewart, I. D., & T. R. Oke, 2006. Methodological concerns surrounding the classification of urban and rural climate stations to define urban heat island magnitude. *Proc. Sixth Int. Conf. on Urban Climate*. Goteborg, Sweden, International Association for Urban Climate, 431–444.
- Taha, H. 1997. "Urban climates and heat islands: albedo, evapotranspiration, and anthropogenic heat." *Energy and Buildings*, 25(2), 99–103.
- Tran, H., D. Uchihama, S. Ochi & Y. Yasuoka. 2006. "Assessment with satellite data of the urban heat island effects in Asian mega cities." *International Journal of Applied Earth Observation and Geoinformation*, 8(1); 34–48.
- Tsang, C. W., K. C. S. Kwok, & P. A. Hitchcock. 2012. "Wind tunnel study of pedestrian level wind environment around tall buildings: Effects of building dimensions, separation and podium." *Building and Environment*, 49, 167–181.
- U.S. Environmental Protection Agency. 2008. Reducing urban heat islands: Compendium of strategies. Draft. <https://www.epa.gov/heat-islands/heat-island-compendium>.
- Van Heerwaarden, C. C., & J. V. Guerau de Arellano, J. V. 2008. "Relative Humidity as an Indicator for Cloud Formation over Heterogeneous Land Surfaces." *Journal of the Atmospheric Sciences*, 65(10), 3263–3277.



- Wang, R., C. Ren, Y. Xu, K. K.-L. Lau, K., & Y. Shi. 2018. "Mapping the local climate zones of urban areas by GIS-based and WUDAPT methods: A case study of Hong Kong." *Urban Climate*, 24, 567–576.
- Weng, Q., D. Lu, & J. Schubring. 2004. "Estimation of land surface temperature–vegetation abundance relationship for urban heat island studies." *Remote Sensing of Environment*, 89(4), 467–483.
- Westerling, A. L., D. R. Cayan, T. J. Brown, B. L. Hall, & L. G. Riddle. 2011. "Climate, Santa Ana Winds and autumn wildfires in southern California." *EOS*, 85(31), 289 – 300.
- Zheng, Y., C. Ren, Y. Xu, R. Wang, J. Ho, K. Lau, & E. Ng. 2018. "GIS-based mapping of Local Climate Zone in the high-density city of Hong Kong." *Urban Climate*, 24, 419-488.

## 5.5. Bibliography

City of Los Angeles, ENERGY AND ENVIRONMENT COMMITTEE. 2016. *Energy and Environment Committee Report relative to the formation of a Committee on Cooling and Urban Heat Impacts, and related matters.*  
<https://cityclerk.lacity.org/lacityclerkconnect/index.cfm?fa=ccfi.viewrecord&cfnumber=15-0198>

Hagen, Bjoern & K. Pijawka. 2017. *Sustainability for the 21st Century: Pathways, Programs, and Policies.* Dubuque, IA: Kendall Hunt Publishing.